(12) INTERNATIONAL APPLICATION PUBLISHED UNDER THE PATENT COOPERATION TREATY (PCT)

(19) World Intellectual Property Organization
International Bureau

(43) International Publication Date
25 June 2020 (25.06.2020)

WIPO | PCT

(10) International Publication Number
WO 2020/127946 A2

(51) International Patent Classification:
Not classified

(21) International Application Number:
PCT/EP2019/086637

(22) International Filing Date:
20 December 2019 (20.12.2019)

(25) Filing Language: English

(26) Publication Language: English

(30) Priority Data:
18214985.6 20 December 2018 (20.12.2018) EP

(71) Applicant: **UNIVERSITÄT BASEL** [CH/CH]; Petersgraben 35, 4001 Basel (CH).

(72) Inventors: **ACETO, Nicola**; Departement Biomedizin, Mattenstrasse 28, 4058 Schweiz (CH). **GKOUNTELA, Sofia**; Departement Biomedizin, Mattenstrasse 28, 4058 Basel (CH).

(74) Agent: **JUNGHANS, Claas**; Schulz Junghans Patentanwälte PartGmbB, Großbeerenstraße 71, 10963 Berlin (DE).

(81) Designated States *(unless otherwise indicated, for every kind of national protection available)*: AE, AG, AL, AM, AO, AT, AU, AZ, BA, BB, BG, BH, BN, BR, BW, BY, BZ, CA, CH, CL, CN, CO, CR, CU, CZ, DE, DJ, DK, DM, DO, DZ, EC, EE, EG, ES, FI, GB, GD, GE, GH, GM, GT, HN, HR, HU, ID, IL, IN, IR, IS, JO, JP, KE, KG, KH, KN, KP, KR, KW, KZ, LA, LC, LK, LR, LS, LU, LY, MA, MD, ME, MG, MK, MN, MW, MX, MY, MZ, NA, NG, NI, NO, NZ, OM, PA, PE, PG, PH, PL, PT, QA, RO, RS, RU, RW, SA, SC, SD, SE, SG, SK, SL, SM, ST, SV, SY, TH, TJ, TM, TN, TR, TT, TZ, UA, UG, US, UZ, VC, VN, ZA, ZM, ZW.

(84) Designated States *(unless otherwise indicated, for every kind of regional protection available)*: ARIPO (BW, GH, GM, KE, LR, LS, MW, MZ, NA, RW, SD, SL, ST, SZ, TZ, UG, ZM, ZW), Eurasian (AM, AZ, BY, KG, KZ, RU, TJ, TM), European (AL, AT, BE, BG, CH, CY, CZ, DE, DK, EE, ES, FI, FR, GB, GR, HR, HU, IE, IS, IT, LT, LU, LV, MC, MK, MT, NL, NO, PL, PT, RO, RS, SE, SI, SK, SM, TR), OAPI (BF, BJ, CF, CG, CI, CM, GA, GN, GQ, GW, KM, ML, MR, NE, SN, TD, TG).

Declarations under Rule 4.17:
— *as to the identity of the inventor (Rule 4.17(i))*
— *as to applicant's entitlement to apply for and be granted a patent (Rule 4.17(ii))*

Published:
— *without international search report and to be republished upon receipt of that report (Rule 48.2(g))*
— *with sequence listing part of description (Rule 5.2(a))*

(54) **Title:** TUBULIN INHIBITORS FOR USE IN THE PREVENTION OR TREATMENT OF METASTASIS

(57) **Abstract:** The invention relates to a tubulin inhibitor for use in the prevention or treatment of metastasis in a cancer patient defined by the presence of CTC clusters in the bloodstream. The tubulin inhibitor of the present invention is selected from a tubulin polymerization inhibitor and a tubulin depolymerization inhibitor. The invention further relates to the use of nucleic acid agents inhibiting the expression of genes related to CTC cluster formation and maintenance.

WO 2020/127946 A2

Tubulin inhibitors for use in the prevention or treatment of metastasis

The present invention relates to tubulin inhibitors for use in the prevention or treatment of metastasis.

This application claims the benefit of the priority of European patent application EP18214985. filed 20 December, 2018, which is incorporated herein in its entirety.

Background

Metastatic spread of cancer, typically to bone, lung, liver and brain, accounts for the vast majority of cancer-related deaths (Nguyen et al., Nat. Rev. Cancer. 2009; 9: 274–284). Epithelial cancer metastasis is thought to involve a series of sequential steps: epithelial-to-mesenchymal transition (EMT) of individual cells within the primary tumor leading to their intravasation into the bloodstream, survival of such circulating tumor cells (CTCs) within the bloodstream (Aceto et al. Trends Cancer 1:44-52, 2015), and finally their extravasation at distant sites, where mesenchymal-to-epithelial transition (MET) culminates in their proliferation as epithelial metastatic deposits (Hanahan and Weinberg, Cell. 2011; 144: 646–674).

Circulating tumor cells are cells that depart from a cancerous tumor and enter the bloodstream, on their way to seeding metastasis (Alix-Panabieres et. al., Clin Chem 59, 110-118, 2013). The analysis of CTCs holds the great promise to dissecting those fundamental features of the metastatic process, enabling the identification of targetable cancer vulnerabilities. Once in the bloodstream, to survive, CTCs need to overcome the loss of adhesion signals from the primary tumor as well as high shear forces that are proper of the circulatory system. In breast cancer, the ability of CTCs to form clusters has been linked to increased metastatic propensity when compared to single CTCs (Aceto et al.; Cell 158, 1110-1122, 2014).

CTCs are found in the blood of cancer patients as single CTCs and CTC clusters (Fidler European Journal of Cancer 9, 223-227 1973; Liotta et al., Cancer Research 36, 889-894 1976), with the latter featuring a higher ability to seed metastasis (Aceto et al. Cell 158, 1110-1122, 2014). Yet, what drives their enhanced metastatic potential and what are the vulnerabilities of clustered CTCs is unknown.

Based on the above-mentioned state of the art, the objective of the present invention is to provide means and methods to prevent and treat metastasis in cancer patients. This objective is attained by the claims of the present specification.

Description

Summary of the invention

The inventors profiled the DNA methylation landscape of single CTCs and CTC-clusters at genome-wide scale, matched within individual cancer patients and human CTC-derived xenografts. They surprisingly found that stemness-related transcription factors orchestrate an OCT4-centric network that is exclusively active in CTC-clusters, and that simultaneously CTC clusters display activation of a SIN3A-dependent cell cycle progression program. This finding demonstrates that the ability of CTCs to form clusters directly impacts on their DNA methylation pattern and results in enhanced stemness and cell cycle progression signals that favor metastasis seeding.

The inventors identified drugs that specifically disrupt CTC-clusters without altering their cellular viability. Upon cluster disruption into single cells, DNA methylation is re-gained at critical sites to shut down the clustering-associated stemness and cell cycle programs, leading to a significant reduction in metastasis-seeding ability.

A first aspect of the invention relates to use of a tubulin inhibitor in the prevention or treatment of metastasis in a cancer patient.

A second aspect of the invention relates to the use of a tubulin inhibitor in the prevention and treatment of venous thromboembolism in cancer patients.

Terms and definitions

For purposes of interpreting this specification, the following definitions will apply and whenever appropriate, terms used in the singular will also include the plural and vice versa. In the event that any definition set forth below conflicts with any document incorporated herein by reference, the definition set forth shall control.

The terms “comprising,” “having,” “containing,” and “including,” and other similar forms, and grammatical equivalents thereof, as used herein, are intended to be equivalent in meaning and to be open ended in that an item or items following any one of these words is not meant to be an exhaustive listing of such item or items, or meant to be limited to only the listed item or items. For example, an article “comprising” components A, B, and C can consist of (i.e., contain only) components A, B, and C, or can contain not only components A, B, and C but also one or more other components. As such, it is intended and understood that “comprises” and similar forms thereof, and grammatical equivalents thereof, include disclosure of embodiments of “consisting essentially of” or “consisting of.”

Where a range of values is provided, it is understood that each intervening value, to the tenth of the unit of the lower limit, unless the context clearly dictate otherwise, between the upper

and lower limit of that range and any other stated or intervening value in that stated range, is encompassed within the disclosure, subject to any specifically excluded limit in the stated range. Where the stated range includes one or both of the limits, ranges excluding either or both of those included limits are also included in the disclosure.

Reference to "about" a value or parameter herein includes (and describes) variations that are directed to that value or parameter per se. For example, description referring to "about X" includes description of "X."

As used herein, including in the appended claims, the singular forms "a," "or," and "the" include plural referents unless the context clearly dictates otherwise.

Unless defined otherwise, all technical and scientific terms used herein have the same meaning as commonly understood by one of ordinary skill in the art (e.g., in cell culture, molecular genetics, nucleic acid chemistry, hybridization techniques and biochemistry). Standard techniques are used for molecular, genetic and biochemical methods (see generally, Sambrook et al., Molecular Cloning: A Laboratory Manual, 4th ed. (2012) Cold Spring Harbor Laboratory Press, Cold Spring Harbor, N.Y. and Ausubel et al., Short Protocols in Molecular Biology (2002) 5th Ed, John Wiley & Sons, Inc.) and chemical methods.

As used herein, the term *treating* or *treatment* of any disease or disorder (e.g. cancer) refers in one embodiment, to ameliorating the disease or disorder (e.g. slowing or arresting or reducing the development of the disease or at least one of the clinical symptoms thereof). In another embodiment "treating" or "treatment" refers to alleviating or ameliorating at least one physical parameter including those which may not be discernible by the patient. In yet another embodiment, "treating" or "treatment" refers to modulating the disease or disorder, either physically, (e.g., stabilization of a discernible symptom), physiologically, (e.g., stabilization of a physical parameter), or both. Methods for assessing treatment and/or prevention of disease are generally known in the art, unless specifically described hereinbelow.

In the context of the present specification, the term *prevention or treatment of metastasis* relates to the process of inhibiting the formation of new metastases that have not existed prior to treatment. This includes but is not limited to reducing the survival rate of cancer cells in the circulation, inhibiting of the extravasation of cancer cells from the blood stream and inhibiting of the seeding process at the site of extravasation.

Detailed description of the invention

A first aspect of the invention relates to a tubulin inhibitor for use in the prevention or treatment of metastasis in a cancer patient. In particular embodiments, the tubulin inhibitor is provided for treatment of a cancer patient characterized by the presence of CTC clusters in the

bloodstream. While any cancer patient, particularly in stages of the disease that lead an elevated risk of metastasis, may be considered at risk of developing metastatic disease, the presence of CTC is a criterion for treatment according to the invention.

In the context of the present specification the term *tubulin* relates to a member of a protein superfamily. Members of the superfamily, in particular α-tubulin and β-tubulin, can combine to form a heterodimer. These α/β-heterodimers can polymerize end-to-end into linear protofilaments. The protofilaments have a positively charged end, which is formed by β-tubulin, and a negatively charged end that is formed by α-tubulin. Protofilaments can attach laterally to each other and form the wall of a tube, which is called a microtubule. Typically, microtubules are formed by thirteen protofilaments, which are required to form the structure of a helix. Other tubulin proteins include γ-tubulin, which is not part of the protofilaments, but forms a γ-tubulin ring that acts as a polymerization seed for α/β-heterodimers. δ and ε tubulin are located at the centrioles and are believed to be involved in the formation of the mitotic spindle.

The term *inhibitor* in the context of the present specification relates to a compound that is able to significantly reduce or completely abolish a physiologic function, activity or synthesis of a target molecule. On an abstract level, inhibition encompasses the interference with the biosynthesis of the target, the prevention of enzyme-substrate binding (the target being the substrate or the enzyme), the prevention of ligand-receptor interaction, etc. In the particular context of the invention, an inhibitor of tubulin includes but is not limited to a compound that significantly reduces or abolishes the polymerization or depolymerization of tubulin heterodimers. Therefore, an inhibitor of tubulin affecting polymerization or depolymerization of tubulin heterodimers can also be a protofilament inhibitor and a microtubule inhibitor, since without the polymerization of tubulin heterodimers no protofilaments can be formed and the assembly of these protofilaments into microtubules does not take place.

In the context of the present specification, the term *prevention of metastasis* relates to the process of inhibiting the formation of new metastases that have not existed prior to treatment. This includes but is not limited to reducing the survival rate of cancer cells in the circulation, inhibiting of the extravasation of cancer cells from the blood stream and inhibiting of the seeding process at the site of extravasation.

In the context of the present specification, the terms *treatment of metastasis* relates to the process of affecting already existing metastases in a way that reduces the size of a metastasis or at least reduces or stops the growth rate of a metastasis. The treatment of a metastasis also includes an effect on a metastasis that prevents a metastasis from segregating factors that negatively affects the host organism, in particular the immune system, or leads to shedding of live cancer cells that may act as seeds for new metastases.

In certain embodiments, the inhibitor according to the invention reduces or prevents the formation of new metastasis. In certain embodiments, the inhibitor according to the invention is useful in the treatment of already existing metastasis. In certain embodiments, the inhibitor according to the invention is active in both prevention and treatment of metastasis.

Without wishing to be bound by theory, the inventors hypothesize that the tubulin inhibitor for use in the prevention or treatment of metastasis according to the invention disrupts CTC clusters, resulting in single CTCs with a significantly decreased potential of metastasis formation as compared to CTC clusters. It is expected that cancer patients with CTC clusters in their bloodstream and/or an increased risk of CTC-clusters will benefit most from the inhibitors of the present invention.

Typically, patients with breast cancer and prostate cancer have the highest incidence of CTC clusters. However, in all cancer types CTC clusters have been detected, therefore the tubulin inhibitor of the current invention is expected to be beneficial to cancer patients in general.

In the context of the present specification, the term *circulating tumor cell* (*CTC)* relates to cells that depart from a cancerous tumor and enter the bloodstream, on their way to seeding metastasis. CTCs can originate from a primary tumor as well as from an established metastasis. Therefore, the inhibitor of the present invention is useful in the treatment of cancer patients regardless of whether they already have an established metastasis or not.

In the context of the present specification, the term *CTC cluster* relates to aggregates of circulating tumor cells typically comprising 2 to 50 CTCs (Aceto et al., Cell 158, 1110–1122, 2014).

The terms *presence of CTC clusters in the bloodstream* relates to cancer patients that have CTC clusters *anywhere* in their bloodstream. In particular large CTC-clusters might be difficult to detect in peripheral blood samples due to the fact that CTC-clusters are rapidly lodged in the capillary bed of blood vessels. Therefore, the absence of detectable CTC-clusters in peripheral blood samples is not necessarily an indicator for the absence of CTC-clusters anywhere in the bloodstream. The skilled person is aware that the location of blood sampling for the detection of CTC-clusters might have to be chosen in dependence of the location of the primary tumor or metastasis that is shedding CTC-clusters.

Methods known to detect and/or isolate CTC clusters in blood samples include physical property-based methods that utilize differences in cell density, size, dielectric properties or mechanical plasticity. For example, a method based on size selection relies on the larger size of CTCs (and CTC clusters) in relation to other blood cells. A non-limiting example of a size based detection/isolation method is the use of the Parsortix device (Xu et al. PLoS One 10,

e0138032, 2015). Another one was published by Shim et al. (Biomicrofluidics 2013, 7(1):11807 doi: 10.1063/1.4774304).

Other known methods for the detection/isolation of CTC-clusters in cancer patients are antibody-based methods. The antibodies used are mainly specific to epithelial cell surface markers that are absent from blood or stroma cells. See also Balasubramanian et al. (PLoS 1 April 12, 2017; https://doi.org/10.1371/journal.pone.0175414).

WO2012 062910 (US9550978, incorporated herein by reference) describes a method of isolating CTC from blood.

In certain embodiments, the tubulin inhibitor for use in the prevention or treatment of metastasis is administered to cancer patients with breast cancer or prostate cancer.

In certain embodiments, the cancer is a solid cancer. A solid cancer is characterized by a tumor that does not contain cysts or liquid areas.

In certain embodiments, the tubulin inhibitor is selected from a tubulin polymerization inhibitor and a tubulin depolymerization inhibitor.

In the context of the present specification, the term *tubulin polymerization* refers to the biochemical process of polymerization of α-tubulin and β-tubulin dimers into linear protofilaments.

The tubulin inhibitors of the present invention interfere with the dynamics of protofilaments/microtubules, by inhibiting the growing (polymerization) or shortening (depolymerization) of the protofilaments/microtubules. Both types of inhibitors would interfere with any cellular process involving microtubules such as mitosis, resulting ultimately in the initiation of apoptosis. Although tubulin inhibitors can already affect the dynamics of microtubules growing and shortening at a dosage lower than the dosage required to initiate apoptosis.

In certain embodiments, the tubulin polymerization inhibitor is selected from a vinca domain binding inhibitor and a colchicine domain binding inhibitor.

The binding sites of tubulin inhibitors to tubulin are named after the class of inhibitor first discovered to engage with this particular binding site. Known binding sites include the vinca domain (or vinca alkaloid binding site), the colchicine domain (or colchicine site), the taxan domain (or taxane site) and the laulimalide domain.

In certain embodiments, the tubulin polymerization inhibitor for use in the prevention or treatment of metastasis is a vinca domain binding inhibitor.

In certain embodiments, the vinca domain binding inhibitor is selected from: vincristine, vinblastine, vinorelbine, vinflunine, cryptophycin 52, halichondrins, dolastatins and hemiasterlines.

Vincristine (22-oxovincaleukoblastine, leurocristine, tradename Oncovin; CAS No. 57-22-7) is a vinca domain binding inhibitor that interferes with tubulin polymerization. Vincristine is approved as a chemotherapeutic agent for treatment in cancer patients.

Vinblastine (CAS No. 865-21-4; tradename Velban) is a vinca domain binding inhibitor and vincristine analog that interferes with tubulin polymerization. Vinblastine is approved as a chemotherapeutic agent for treatment in cancer patients.

Vinorelbine (tradename Navelbine; CAS No. 71486-22-1) is a vinca domain binding inhibitor and vincristine analog that interferes with tubulin polymerization. Vinorelbine is approved as a chemotherapeutic agent for treatment in cancer patients.

Vinflunine (tradename Javlor, CAS No. 162652-95-1) is a vinca domain binding inhibitor that interferes with tubulin polymerization. Vinflunine is approved as a chemotherapeutic agent for treatment in cancer patients.

Cryptophycin 52 is a synthetic derivative of cryptophycin 1, a potent tubulin inhibitor of the class of vinca domain binding inhibitor isolated from cyanobacteria.

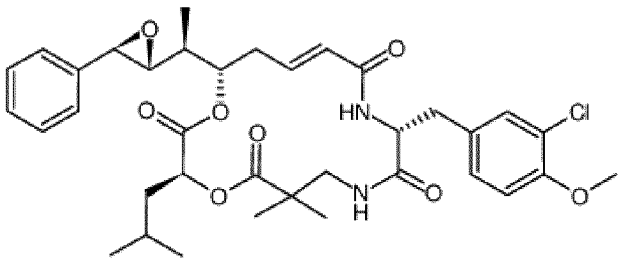

cryptophycin 52 (CAS 186256-67-7)

Halichondrins are large polyether macrolides originally isolated from the marine sponge *Halichondria okadai*. Examples of halichondrins are the naturally occurring halichondrin B (CAS 103614-76-2) or the synthetic analogue eribulin (CAS 253128-41-5).

In certain embodiments, the colchicine domain binding inhibitor is selected from: colchicine, podophyllotoxin, rigosertib, steganacin, ABT-751, combretastatins and 2-methoxyestradiol.

Colchicine is a naturally occurring tubulin binding antimitotic compound originally isolated from plants of the genus *Colchicum*. Colchicine inhibits microtubule polymerization by binding to tubulin at its colchicine domain binding site.

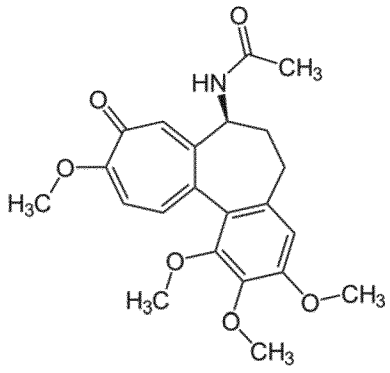

colchicine (CAS 64-86-8).

Podophyllotoxin is a naturally occurring lignan originally isolated from the roots of plants of the genus *podophyllum*. Podophyllotoxin inhibits microtubule polymerization by binding to tubulin at its colchicine domain binding site and thereby destabilizes microtubules.

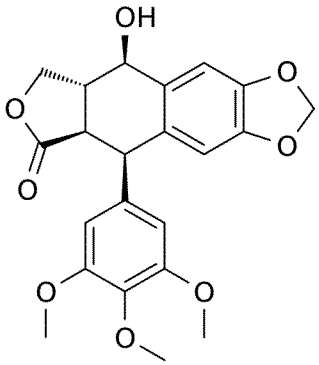

podophyllotocin (CAS 518-28-5).

Rigosertib (also known as ON-01910) is a small molecule compound that is a colchicine site binding inhibitor of tubulin polymerization (Jost et al. Molecular Cell 68, 210–223, October 5, 2017). In addition, rigosertib is also a dual kinase inhibitor that simultaneously inhibits the phosphoinositide 3-kinase (PI3K) and polo-like kinase 1 (PLK-1) pathway.

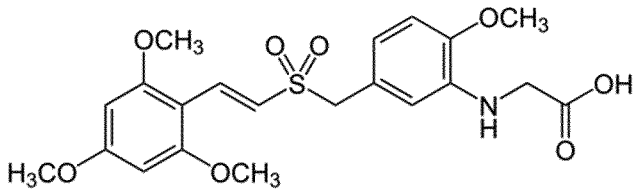

rigosertib (CAS 1225497-78-8).

Steganancin is a naturally occurring lignan originally isolated from *Steganotaenia araliacea*. Steganancin inhibits microtubule polymerization by binding to tubulin at its colchicine domain binding site and thereby destabilizes microtubules.

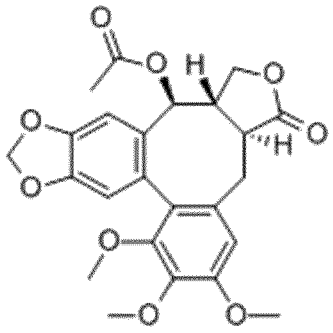

steganacin (CAS 41451-68-7)

ABT 751 inhibits microtubule polymerization by binding to tubulin at its colchicine domain binding site and thereby destabilizes microtubules.

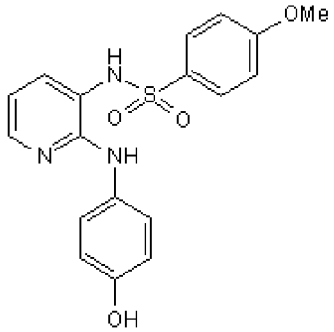

ABT 751 (CAS 141430-65-1)

Combrestatin is a dihydrostilbenoid originally isolated from *Combretum caffrum*. Combrestatin inhibits microtubule polymerization by binding to tubulin at its colchicine domain binding site and thereby destabilizes microtubules.

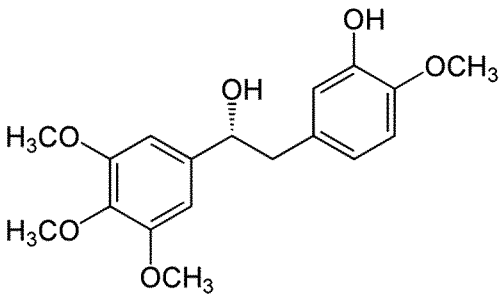

combrestatin (CAS 82855-09-2)

Fenbendazole is a benzimidazole used as an anthelmintic for gastrointestinal parasites. Fenbendazole inhibits microtubule polymerization by binding to tubulin at its colchicine domain binding site and thereby destabilizes microtubules.

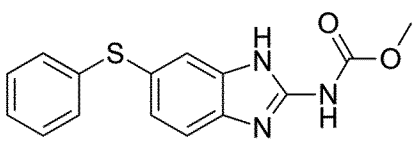

fenbendazole (CAS 43210-67-9)

Oxibendazole is a benzimidazole used as an anthelmintic for gastrointestinal parasites. Oxibendazole inhibits microtubule polymerization by binding to tubulin at its colchicine domain binding site and thereby destabilizes microtubules.

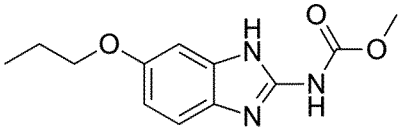

oxibendazole (CAS 20559-55-1)

Albendazole is a benzimidazole used as an anthelmintic for gastrointestinal parasites. Albendazole inhibits microtubule polymerization by binding to tubulin at its colchicine domain binding site and thereby destabilizes microtubules.

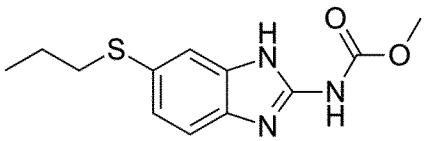

albendazole (CAS 54965-21-8)

2-Methoxyestradiol is a metabolite of estradiol. 2-Methoxyestradiol inhibits microtubule polymerization by binding to tubulin at its colchicine domain binding site and thereby destabilizes microtubules.

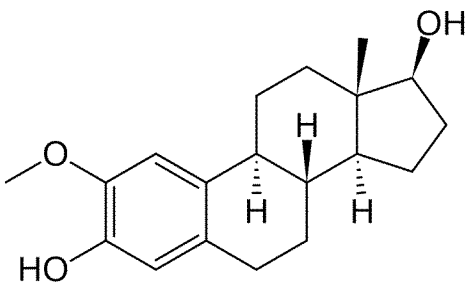

2-Methoxyestradiol (CAS 362-07-2)

In certain embodiments, the tubulin depolymerization inhibitor is selected from a taxan domain binding inhibitor and a laulimalide binding inhibitor.

In certain embodiments, the taxan domain binding inhibitor is selected from paclitaxel, docetaxel, epothilone and discodermolide. Paclitaxel is a naturally occurring compound originally isolated from the bark of the pacif yew tree. Paclitaxel inhibits microtubule depolymerization by binding to tubulin at its taxan domain binding site and thereby stabilizes microtubules.

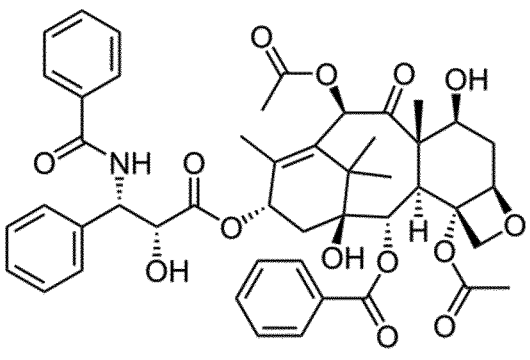

paclitacel (CAS 33069-62-4)

Docetaxel is a semi-synthetic analogue of paclitaxel. Docetaxel inhibits microtubule depolymerization by binding to tubulin at its taxan domain binding site and thereby stabilizes microtubules.

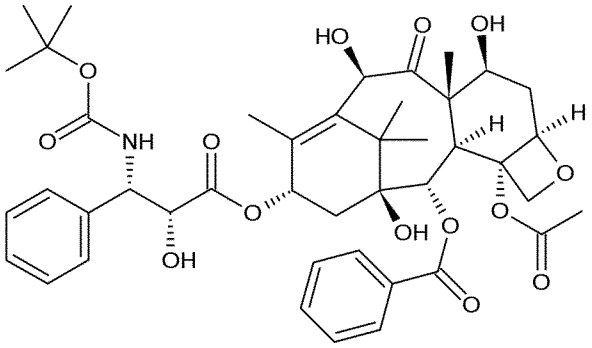

docetaxel (CAS 114977-28-5).

Epothilones are a class of taxane binding site inhibitors. Epothilones inhibit microtubule depolymerization by binding to tubulin at its taxan domain binding site and thereby stabilize microtubules. Example of epothilones are epothilone A (CAS 152044-53-6), epothilone B (CAS 152044-54-7), epothilone C, epothilone D (CAS 189453-10-9), epothilone E and epothilone F.

Discodermolide is a naturally occurring compound originally isolated from the deep-sea sponge *Discodermia dissolute.* Discodermolide inhibits microtubule depolymerization by binding to tubulin at its taxan domain binding site and thereby stabilizes microtubules.

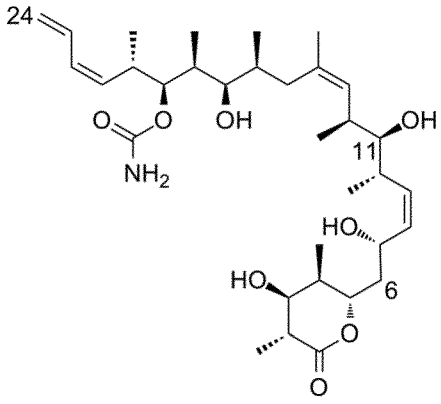

discodermolide (CAS 127943-53-7)

In certain embodiments, the laulimalide binding inhibitor is selected from laulimalide and peloruside A. Laulimalide is naturally occurring compound originally isolated from the marine sponge *Cacospongia mycofijiensis*. Laulimalide inhibits microtubule depolymerization by binding to tubulin at its laulilamide domain binding site and thereby stabilizes microtubules.

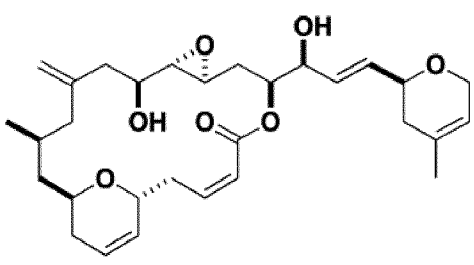

laulimalide

In certain embodiments according to any aspects and embodiments of the present invention the tubulin inhibitor can be formulated as a pharmaceutically acceptable salt.

Pharmaceutically acceptable salts comprise the ionized drug and an oppositely charged counterion. Non-limiting examples of pharmaceutically acceptable anionic salt forms include acetate, benzoate, besylate, bitatrate, bromide, carbonate, chloride, citrate, edetate, edisylate, embonate, estolate, fumarate, gluceptate, gluconate, hydrobromide, hydrochloride, iodide, lactate, lactobionate, malate, maleate, mandelate, mesylate, methyl bromide, methyl sulfate, mucate, napsylate, nitrate, pamoate, phosphate, diphosphate, salicylate, disalicylate, stearate, succinate, sulfate, tartrate, tosylate, triethiodide and valerate. Non-limiting examples of pharmaceutically acceptable cationic salt forms include aluminium, benzathine, calcium, ethylene diamine, lysine, magnesium, meglumine, potassium, procaine, sodium, tromethamine and zinc.

In certain embodiments, the tubulin inhibitor for use in the prevention or treatment of metastasis is effective in the disruption of CTC clusters.

Compared to single circulating tumor cells , CTC clusters have a higher potential for metastasis seeding. Therefore, the ability of the tubulin inhibitor of the present invention to disrupt the CTC clusters into single CTCs is advantageous in the prevention and treatment of cancer patients.

In certain embodiments, the tubulin inhibitor additionally comprises a dual kinase inhibitory activity. In other words, the tubulin inhibitor of the present invention additionally is capable of inhibiting two different kinases. In certain embodiments, the two inhibited kinases belong to different kinase families.

In certain embodiments, the tubulin inhibitor with dual kinase inhibitory activity is an inhibitor of the PI3K and PLK1 pathway.

In certain embodiments, the tubulin inhibitor with dual kinase inhibitory activity is binding to the substrate binding site of its kinase targets.

In certain embodiments, the tubulin inhibitor with dual kinase inhibitory activity is binding to the substrate binding site of PI3K and PLK1.

In certain embodiments, the tubulin inhibitor with an additional dual kinase inhibiting property is rigosertib.

Another aspect of the invention relates to a tubulin inhibitor according to the first aspect of the invention for use in the prevention and treatment of venous thromboembolism in cancer patients.

Presence of CTCs in patients with cancer is associated with an increased risk of venous thromboembolism. Without wishing to be bound by theory this is presumably due to activation

of coagulation via CTC-cluster interaction with coagulation or tissue factors in the blood circulation and/or other cell types such as platelets and endothelial cells (Bystricky et al., Critical Reviews in Oncology/Hematology 114: 33-42, 2017).

The tubulin inhibitors of the present invention significantly reduce CTC cluster size and are therefore also able to reduce the incidence of venous thromboembolism in cancer patients.

All embodiments relating to the tubulin inhibitor of the first aspect of the invention also relate to the second aspect of the invention.

Another aspect of the invention relates to the use of the tubulin inhibitor as characterized above in the manufacture of a medicament for cancer treatment as outlined above. Alternatively, the invention relates to methods for cancer treatment. In such methods, an effective amount of the compound described herein (including a dosage form or formulation as described), is administered to a subject in need thereof, thereby treating the cancer or preventing the spread or recurrence of metastasis.

Pharmaceutical Compositions and Administration

Another aspect of the invention relates to a pharmaceutical composition comprising a compound of the present invention, or a pharmaceutically acceptable salt thereof, and a pharmaceutically acceptable carrier.

In certain embodiments, the tubulin inhibitor according to the invention and any of its aspects and embodimentsis formulated as a dosage form for enteral administration, such as nasal, buccal, rectal, transdermal or oral administration, or as an inhalation form or suppository. Alternatively, parenteral administration may be used, such as subcutaneous, intravenous, intrahepatic or intramuscular injection forms. Optionally, a pharmaceutically acceptable carrier and/or excipient may be present.

In certain embodiments of the invention, the compound of the present invention is typically formulated into pharmaceutical dosage forms to provide an easily controllable dosage of the drug and to give the patient an elegant and easily handleable product.

In embodiments of the invention relating to topical uses of the compounds of the invention, the pharmaceutical composition is formulated in a way that is suitable for topical administration such as aqueous solutions, suspensions, ointments, creams, gels or sprayable formulations, e.g., for delivery by aerosol or the like, comprising the active ingredient together with one or more of solubilizers, stabilizers, tonicity enhancing agents, buffers and preservatives that are known to those skilled in the art.

The pharmaceutical composition can be formulated for oral administration, parenteral administration, or rectal administration. In addition, the pharmaceutical compositions of the

present invention can be made up in a solid form (including without limitation capsules, tablets, pills, granules, powders or suppositories), or in a liquid form (including without limitation solutions, suspensions or emulsions).

The dosage regimen for the compounds of the present invention will vary depending upon known factors, such as the pharmacodynamic characteristics of the particular agent and its mode and route of administration; the species, age, sex, health, medical condition, and weight of the recipient; the nature and extent of the symptoms; the kind of concurrent treatment; the frequency of treatment; the route of administration, the renal and hepatic function of the patient, and the effect desired. In certain embodiments, the compounds of the invention may be administered in a single daily dose, or the total daily dosage may be administered in divided doses of two, three, or four times daily.

The pharmaceutical compositions of the present invention can be subjected to conventional pharmaceutical operations such as sterilization and/or can contain conventional inert diluents, lubricating agents, or buffering agents, as well as adjuvants, such as preservatives, stabilizers, wetting agents, emulsifiers and buffers, etc. They may be produced by standard processes, for instance by conventional mixing, granulating, dissolving or lyophilizing processes. Many such procedures and methods for preparing pharmaceutical compositions are known in the art, see for example L. Lachman et al. The Theory and Practice of Industrial Pharmacy, 4th Ed, 2013 (ISBN 8123922892).

The invention is further illustrated by the following examples and figures, from which further embodiments and advantages can be drawn. These examples are meant to illustrate the invention but not to limit its scope.

Brief description of the figures

Fig. 1 shows DNA-methylation analysis of human single CTCs and CTC cluster A) staining of live CTCs for cell surface expression of EpCAM, HER2, and EGFR (Alexa488- or FITC-conjugated), and counterstained with antibodies against CD45 to identify contaminant leukocytes. B) Principal component analysis mainly separated CTCs based on the patient of origin, with CTC clusters (circles) being more heterogeneous compared to single CTCs (triangle). C) NES score representing enrichment of transcription factor binding sites (TFBSs) in CTC-cluster hypomentylated regions (n=1305) and single CTC hypomethylated regions (n=2042), identified using i-cisTarget. D) Gene ontology (GO) enrichment analysis for 166 genes located at hypomethylated regions in CTC clusters ($p=< 0.05$).

Fig. 2 shows DNA-methylation analysis of mouse xenograft single CTCs and CTC cluster A) NES score representing enrichment of transcription factor binding sites (TFBSs) in

CTC-cluster hypomethylated regions (n=909) and single CTC hypomethylated regions (n=521), identified using i-cisTarget. B) Only a very small subset of TFBSs are preferentially hypomethylated in either single CTCs (n=13) or CTC clusters (n=9)

Fig. 3 shows RNA Sequencing analysis of single CTCs and CTC clusters isolated from breast cancer patients A) Network analysis of transcripts identified in the CTC cluster-associated modules B) Gene regulatory network analysis showing transcription factor dependence on TFs SIN3A, OCT4 and CBFB that also display hypomethylated binding sites. C) RNA-sequencing analysis of xenograft-derived CTC clusters showed additionally to those genes found enriched in patient's CTC clusters TFs with significantly hypomethylated binding sites such as SIN3A, NANOG, SOX2, RORA, FOXO1 and BHLHE40. D) Gene ontology (GO) enrichment analysis for genes located at hypomethylated regions in CTC clusters. E) Transcription factor target gene analysis for single CTCs further confirmed the activity of c-MYC, as well as E2F4.

Fig. 4 shows a screen for FDA approved compounds that dissociate CTC clusters. A) Left panels: representative images of steady state "unfiltered" and 40 µM-filtered BR16 cells stained with Hoechst and TMRM. Images are taken with a high-content screening microscope. Right panels: representative images of single and clustered CTCs outline based on nuclei proximity (derived from respective left panel images) as determined using Colombus Image data analysis system. The bar graphs show the mean cluster size (area in µM2) and percentage (%) of viability of unfiltered versus filtered BR16 cells (n=3; NS: not significant; ***p<0.001). B) Top panel: the plot shows mean cluster size of BR16 cells treated with each of the 39 cluster-targeting compounds at 4 different concentrations: 5 µM, 1 µM, 0.5 µM, and 0.1 µM. Cluster-targeting compounds include inhibitors of Na^+/K^+ ATPase (n=6), HDAC (n=2), nucleotide biosynthesis (n=5), kinase (n=4), GPCR (n=2), cholesterol biosynthesis (n=1) and nuclear export (n=1) as well as tubulin (n=9) and DNA binding (n=8) compounds and antibiotics (n=1). BR16 cells that were untreated or untreated and 40 µM-filtered are shown as controls for comparison. The average value of two independent measurements is shown. Bottom panel: heatmap showing number of nuclei, average TMRM intensity and % viability for BR16 cells treated with cluster-targeting compounds at the indicated concentrations.

Fig. 5 shows the effect of 17-day in vitro treatment of BR16 and BRx50 cell line with 50 nM, 20 nM, 10 nM, 5 nM and 1 nM concentration of digitoxin, ouabain octahydrate and rigosertib on reducing cluster size, number of nuclei, TMRM intensity and % viability relative to untreated or untreated and further 40 µM filtered cells.

Fig. 6: shows the effect of treatment of CTC-derived cell lines with digitoxin and ouabain. (A) Western blot for CLDN3, CLDN4 and GAPDH on BR16 cells with double knockout (KO) of CLDN3 and CLDN4. KO=Knockout. (B) Plot showing the reduction in mean cluster size (area in µm2) of the CLDN3/4 double KO BR16 cells, relative to control BR16 cells. *P<0.05; **P<0.01 by Student's t test. Error bars represent S.E.M.

Examples

Abnormal DNA methylation patterns, including both genome-wide hypomethylation and hypermethylation have been associated with several human cancers (Klutstein et al., Cancer research 76, 3446-3450, 2016; Ehrlich Epigenomics 1, 239-259, 2009; Ehrlich, M. Oncogene 21, 5400-5413, 2002; Feinberg et al., Nat Rev Genet 7, 21-33, 2006). Generally, these cancer-associated epigenetic modifications appear to affect distinct genomic areas, with hypomethylation favoring regulatory and repetitive elements, versus hypermethylation being more frequent in CpG islands (Ehrlich, M. Oncogene 21, 5400-5413, 2002). Yet, both modifications have the ability to alter the expression of neighboring genes and to contribute to the cancer phenotype (Klutstein et al., Cancer research 76, 3446-3450, 2016; Ehrlich Epigenomics 1, 239-259, 2009). With regard to regulatory elements, loss of DNA methylation at transcription factor binding sites (TFBSs) can designate active transcription factor (TF) networks, or networks that are primed for activation at later stages, e.g. during derivation of induced pluripotent stem cells from differentiated cells (Lee et al., Nat Commun 5, 5619, 2014) or cancer progression. However, the forces that shape the DNA methylome in breast cancer patients and whether distinct DNA methylation patterns dictate the metastatic potential of CTCs is unknown.

DNA-methylation pattern of circulating tumor cells (CTC) and CTC clusters from breast cancer patients

The inventors sought to identify active transcription factor networks by means of accessible TFBSs of single and clustered human breast CTCs, matched within individual liquid biopsies, through a genome-wide single cell-resolution DNA methylation analysis (bisulfite sequencing). To this end, blood samples were drawn from four patients with progressive metastatic breast cancer (Table 1) and processed with Parsortix (Xu et al. PLoS One 10, e0138032, 2015), a microfluidic device that allows a size-based, antigen-agnostic enrichment of CTCs from unmanipulated blood samples. Upon capture, live CTCs were stained for cell surface expression of EpCAM, HER2, and EGFR (Alexa488- or FITC-conjugated), and counterstained with antibodies against CD45 to identify contaminant leukocytes (Fig. 1a). Upon staining verification, a total of 18 marker-positive single CTCs and 24 marker-positive CTC clusters (mean of 5±2.58 single CTCs and 6±4.24 CTC clusters per patient) were then individually

micromanipulated (CellCelector) and deposited in lysis buffer for single cell whole-genome bisulfite sequencing (Farlik et al., Cell Rep 10, 1386-1397, 2015; Farlik et al., Cell Stem Cell 19, 808-822, 2016).

Table 1: Breast cancer patient information at the time of CTC collection for WGBS and/or RNA sequencing analysis

Patient ID	Age	Stage	% ER^+/PR^+	HER2	Metastatic Sites	# of detected CTCs
BR7	42	IV	90/90	-	Bone	6 single, 11 clusters
BR16	49	IV	100/75	-	Bone, Liver, Peritoneum, Meningeosis	8 single, 3 clusters
BR23	64	IV	100/0	-	Peritoneum, Uterus, Ovaries	2 single, 8 clusters 1 single, 4 clusters
BR61	63	IV	60/0	-	Bone, Soft Tissues, Lymphnodes	4 single, 2 clusters 9 single, 9 clusters
BR11	58	IV	0/0	-	Skin, Liver	11 singles; 2 clusters
BR39	53	IV	60/30	-	Bone, Liver, Pleura	14 singles, 7 clusters
BR53	59	IV	>1/0	-	CNS, Lung, Liver, Peritoneum	1 cluster
BR57	56	IV	95/5	-	Bone, Liver, Lymphnodes	13 single, 1 cluster

Principal component analysis (PCA) mainly separated CTCs based on the patient of origin, with CTC clusters being more heterogeneous compared to single CTCs (Fig. 1b). To identify differentially methylated regions (DMRs) between single CTCs and CTC clusters, methylation in 5kb windows that are common between at least two different samples in each group was evaluated, and 3'347 DMRs were identified, with a ≥80% methylation difference between single CTCs and CTC clusters. Of these, 1'305 DMRs were hypomethylated in CTC clusters and 2'042 were hypomethylated in single CTCs. DMRs were analyzed with i-cisTarget, an integrative genomics method that predicts cis regulatory features in co-regulated sequences (Herrmann et al., Nucleic Acids Res 40, e114, 2012). Within CTC cluster hypomethylated DMRs, a significant enrichment for several TFBSs was found, including stemness-related TFs such as OCT4 and STAT3 (Fig. 1c). In contrast, hypomethylated DMRs in single CTCs were enriched in TFBSs for TF such as MEF2C and SOX18 (Fig. 1c). The genomic regions enrichment of annotations tool (GREAT) (McLean et al. Nat Biotechnol 28, 495-501, 2010) was used to identify specific genes that were associated with hypomethylated regions in CTC clusters. Using an association rule of basal plus 50kb maximum extension, this analysis

revealed 166 genes that are associated with gene ontology (GO) categories related to processes that involve cell-cell junction and membrane receptor activity such as adherens junctions, NMDA receptor activity and lipid transport, as well as immune response, including NK cell activation and leukocyte apoptosis (Fig. 1d and Table 2). As a parallel approach, global DNA methylation differences were assessed at TFBSs (Farlik et al., Cell Stem Cell 19, 808-822, 2016) and found OCT4 binding sites to be consistently hypomethylated in CTC clusters (Table 3). Binding sites for other pluripotency-related TFs such as SOX2 and ESRRB were also hypomethylated, as well as binding sites for cell cycle progression-related TFs such as SIN3A (Table 3). In contrast, in single CTCs, with this approach hypomethylation at TFBSs for several TFs were observed including c-MYC and E2F4 (Table 3). Together, the results suggest that CTC clusters display an accessible stemness-related OCT4-centric TF network as well as a cell cycle progression-related SIN3A-centric TF network, paralleling embryonic stem cells (ESCs) biology, whereby these networks simultaneously regulate self-renewal and proliferation (Niwa, Development 134, 635-646, 2007; Kim et al., Cell 132, 1049-1061, 2008; van den Berg et al., Cell Stem Cell 6, 369-381, 2010). Differently, single CTCs appear to be characterized by a c-MYC-centric network, which is commonly enriched in various cancers, yet largely independent of a core pluripotency network and more involved in the regulation of genes associated with metabolism (Kim et al., Cell 132, 1049-1061, 2008; Kim et al. Cell 143, 313-324, 2010).

Table 2: Genes identified by GREAT as associated with CTC cluster hypomethylated DMRs in breast cancer patients.

ACER3	ENSG00000261833	MBTPS2	PVRL3
ADAMTS18	ENSG00000269964	MEF2C	RAB3C
ALG10	EPS8	MLIP	RELN
ALG6	EYA4	MMP26	RERG
AMBN	FAM174A	MRAP2	RGPD4
ANGPT1	FAM98B	MSC	RGS7BP
ANGPTL1	FERMT1	MUC7	RHOJ
ANO3	FRG2C	MYH4	RHOXF2B
AR	GALNTL6	MYH8	RORB
ARHGAP6	GAP43	NAALADL2	SATB1
ASXL3	GCC1	NALCN	SDIM1
B3GAT2	GOLGA8B	NAP1L6	SKAP2
BTNL3	GOLGA8H	NCAM1	SLCO1B1
C10orf25	GOLGA8Q	NEGR1	SLIT2
C10orf35	GPR85	NEUROG3	SNX19
C4orf3	GRXCR1	NLGN1	SPANXC
C4orf40	GUCY2F	NME8	SPATA22
CA10	HCN1	NPC2	STARD4
CAPN6	HNRNPA1L2	NPR3	STXBP5L

CCDC39	HYDIN	NR2F2	SYNDIG1L
CCDC66	IFNA14	NRXN3	TMEM64
CDH6	IFNA5	NUDT10	TMPRSS11F
CDH9	IFNG	NXT2	TPH2
CENPE	INSIG2	OPRM1	TRIM49D1
CFHR3	INSL6	OR13H1	TRIM64B
CHCHD4	IRS2	OR1E2	TRPC6
CLEC2A	ITGBL1	OR4D5	TSKU
CLSTN3	ITM2A	OR4M1	UBE2E2
CNTNAP2	JRKL	OR4N2	UGT2A2
CNTNAP5	KCNIP4	OR4P4	UGT8
COL11A1	KCTD8	OR8D4	UPK1B
COL12A1	KL	PABPC5	USP53
CRB1	KLHL1	PDE10A	VAMP7
CTAG1B	KLRF2	PDE4B	VGLL2
DACH2	LCA5	PDHA2	XXYLT1
DGKH	LDOC1	PEX5	ZBTB41
DHRS4L2	LGALS14	PLXDC2	ZKSCAN7
DHRS7	LGALS16	POU3F4	ZNF208
DNAH6	LPAR4	PPP1R3A	ZNF676
ENAM	LRRC16B	PRL	ZNF729
ENSG00000176134	LUM	PRSS37	
ENSG00000257062	MAX	PTPRZ1	

Association rule: Basal+extension: 5000 bp upstream, 1000 bp downstream, 50000 bp max extension, curated regulatory domains included.

Table 3: Global methylation differences at TFBS in single CTCs versus CTC clusters

Hypomethylated in CTC cluster		Hypomethylated in single CTC
SOX2	SP2	POL2
STAT1	BCL3	TLX1
CTCF	YY1	c−MYC
BRCA1	MAFF	POL2
ESRRB	RAD21	KAP1
MAFK	TAL1	PGC1A
CTCF	EGR−1	MBD4
YY1	TR4	RUNX1
EZH2	NFKB	IRF3
STAT1	EZH2	MYB
POL2	OCT4	JUND
MYB	NFKB	IRF3
SIN3A	LYL1	DDIT3
BCLAF1		POL2
ZBTB33		NFKB
POL2		BRF2
ATF3		E2F4
NR2F2		PAX5
PML		POL2
p300		ZNF

Hypomethylated in CTC cluster	Hypomethylated in single CTC
RAD21	CTCF

DNA-methylation pattern of circulating tumor cells (CTC) and CTC clusters from an established mouse model

Spontaneously-generated GFP-labeled single CTCs and CTC clusters from three independent mouse xenograft models, including two human breast CTC-derived cell lines (BR16 and BRx50) as well as the breast cancer cell line MDA-MB 231 (lung metastatic variant, referred to as LM2) (Yu et al., Science 345, 216-220, 2014; Minn et al. Nature 436, 518-524, 2005), were isolated to test the robustness of the findings. In this setting, 71 single CTCs and 47 CTC clusters (Table 4) were individually micromanipulated and processed for single cell whole-genome bisulfite sequencing (Farlik et al., Cell Rep 10, 1386-1397, 2015; Farlik et al., Cell Stem Cell 19, 808-822, 2016). Similarly, to patient's CTCs, PCA analysis of xenograft CTCs segregated them primarily based on the cell line of origin, yet displaying an overall higher homogeneity of the samples compared to patient's CTCs. DMRs with a >70% methylation difference between single CTCs and CTC clusters were assessed and a total of 1'430 DMRs were found, of which 909 are hypomethylated in CTC clusters and 521 are hypomethylated in single CTCs. Using i-cisTarget analysis, 40 TFBSs were identified that were hypomethylated in CTC clusters, and 74 TFBSs that were hypomethylated in single CTCs (Fig 2a). Interestingly, in line with patient data, both the binding sites for the OCT4-centric TF network, such as those belonging to SOX2, NANOG, STAT3 and REX1, and that of SIN3A were hypomethylated in xenograft CTC clusters. In contrast to patient CTCs though, the stemness-related TF network accessibility seemed to be regulated by localized DNA methylation remodeling at DMRs rather than affecting the global DNA methylation profile of CTCs. This was corroborated by the finding that only a handful of TFBSs are preferentially hypomethylated in either single CTCs (n=13) or CTC clusters (n=9) (Fig 2b). Thus, distinct DNA methylation profiles of patient and xenograft CTCs seem to reflect their clustering status. It also indicates that, in breast cancer, interplay between methylation dynamics and phenotypic properties of CTCs occurs, and that CTC clustering is associated to an epigenetic predisposition to undergo stemness-related processes and cell cycle progression.

Table 4: Number of single CTCs and CTC clusters isolated per BR16, BRx50 and LM2 injected xenograft mouse models and used for WGBS or RNA sequencing analysis.

Mouse ID	Number of CTCs	WGBS	RNA-Seq
BR16-1	10 single; 7 clusters	✓	-
BR16-2	23 single; 19 clusters	✓	-
BR16-3	6 single; 15 clusters	-	✓
BR16-4	16 single, 23 clusters	-	✓
BR16-5	10 singles, 4 clusters	-	✓
BRX50-1	10 single, 3 clusters	✓	-
BRX50-2	2 single, 1 cluster	✓	-
BRX50-3	4 single, 2 clusters	-	✓
LM2-1	16 single; 10 clusters	✓	-
LM2-2	10 single; 7 clusters	✓	-
LM2-3	5 singles; 3 clusters	-	✓
LM2-4	5 singles; 2 clusters	-	✓
LM2-5	3 singles; 5 clusters	-	✓

Stem-cell like related transcription factor networks

To identify whether the accessible stemness-related TFs networks are also transcriptionally active, the inventors performed single cell-resolution RNA-Sequencing analysis of 48 single CTCs and 24 CTC clusters, matched within individual liquid biopsies and isolated from 6 breast cancer patients with progressive metastatic disease, and of 49 single CTCs and 54 CTC clusters isolated from the three xenograft mouse models (Table 4). A set of 335 genes that were previously shown to be consistently upregulated in mouse and human embryonic stem cells and embryonal carcinoma cells as opposed to their differentiated counterparts was further investigated (Wong et al. Cell Stem Cell 2, 333-344, 2008). A subset of 301 of these 335 genes were found to be expressed in the CTC samples. With these genes, a weighted gene co-expression network analysis (WGCNA) was performed and four expression modules in human breast cancer samples (blue, grey, turquoise and brown) and four expression modules in xenograft CTC clusters were identified (green, yellow, orange, purple), revealing module-trait relationships in CTCs. Particularly, 85 transcripts enriched in patient CTC clusters and 153 in xenograft CTC clusters were identified (Table 5 and 6) with 90% overlap between patient and xenograft CTC-cluster-enriched stemness-related transcripts. Interestingly, transcripts enriched in patient's CTC clusters, as well as those that overlap between patients and xenografts, are mostly involved in cell cycle progression as judged by their network analysis

(Fig. 3a), while TF target gene analysis confirmed, among others, activity of TFs SIN3A, OCT4 and CBFB with significantly hypomethylated binding sites (Fig. 3b). In a similar fashion, in xenograft-derived CTC clusters, additionally to those genes found enriched in patient's CTC clusters, TF target gene analysis highlighted the activity of OCT4 including TFs with significantly hypomethylated binding sites such as SIN3A, NANOG, SOX2, RORA, FOXO1 and BHLHE40 (Fig 3c). TF target gene analysis for single CTCs further confirmed the activity of c-MYC, as well as p53 and E2F4, among others (Fig. 3e). Together, the gene expression data supports the model proposed with DNA methylation analysis, demonstrating that CTC clusters are primed for an OCT4-centric stemness-related TF network and display activation of a SIN3A-dependent cell cycle progression program. Activation of these programs plays a role in determining the metastasis-seeding ability of CTC clusters.

DNA methylation patterns in CTC clusters shape an accessible and active transcription factor network that gives a proliferation advantage in CTC clusters over single CTCs in breast cancer patients. The forces that shape the DNA methylome involve both global differences at TFBSs as well as localized events that mediate response to environmental cues and phenotypic properties. Harnessing the ability to dynamically shape the DNA methylome in response to environmental stimuli can be exploited therapeutically by repurposing FDA approved compounds.

Table 5: Weighted gene co-expression network analysis (WGCNA) of stemness related genes in breast cancer patient CTCs and distribution of genes per expression module

Blue Module			
BIRC5	MYBL2	EXO1	COQ3
BLM	NEK2	AURKB	ERCC6L
BUB1	PCNA	TRIP13	CDCA8
BUB1B	PLK1	GNA14	RAD18
CCNA2	POLD1	NCAPD2	LSM2
CCNF	POLE2	CHAF1A	ANP32E
CDC6	PRIM1	SMC4	CDCA3
CDC20	PRIM2	NDC80	CDCA7
CDKN3	RFC3	SMC2	CDCA5
CHEK1	RPA2	SPAG5	
CKS2	RRM2	PLK4	
DNMT1	SLC16A1	WDHD1	
HELLS	AURKA	CHEK2	
HMGB2	TCF19	NCAPH	
LMNB1	TOP2A	CKAP2	
MAD2L1	TTK	RACGAP1	
MCM2	VRK1	NUSAP1	
MCM3	CDC7	GTSE1	
MCM5	CCNB2	DTL	

Grey Module			
ALDOC	GLDC	ELOVL6	TMEFF1

BCAT1	E2F3	MID1IP1	U2AF1
CCND2	PABPC1	PIPOX	GSPT2
CDKN1C	ACAD8	PRMT3	RAB34
FGFR1	LSM10	DPP3	

Brown Module			
SLC25A5	GLO1	PSMA7	EIF2S2
ALDH7A1	HSPE1	RPA3	GNPDA1
ATP5J	IARS	RPL13	LYPLA1
ATP5O	RPSA	RPL22	MTHFD2
BTF3	NAP1L1	RPL27A	RUVBL2
CKS1B	NDUFA9	RPS3	EBNA1BP2
COX5B	NDUFB7	RPS5	LSM5
CTNNA1	NDUFB8	RPS8	TIMM13
DTYMK	RPL10A	RPS12	TIMM8B
ECHS1	NME2	RPS16	CYCS
EIF4EBP1	PA2G4	RPS19	NT5DC2
ENO1	PRDX1	RPS23	THOC3
ETFA	POLR2F	RPS27	FAM136A
FDPS	PRPS1	SNRPA	NDUFA11

Turqoise Module			
ABCB7	NDUFAB1	ZNF22	STOML2
ADH5	NDUFS2	DAP3	GMNN
PARP1	NME4	DEK	MRPL4
ADSL	NONO	CLPP	UTP18
APEX1	NTHL1	TEAD2	MRPS2
BAX	PDCD2	NIPSNAP1	MRTO4
CCND1	PDHA1	HAT1	HN1
SERPINH1	PHB	RUVBL1	HSPA14
CCNC	PPM1G	BANF1	MRPL37
CDC34	PPP4C	PROM1	MRPS17
CTSC	MAPK13	DDX18	NIP7
RCC1	PSMB5	BUB3	AMOTL2
CRABP2	PSMB6	EEF1E1	POLR3K
CSE1L	RAD23B	PDIA4	WBP11
CSRP2	RCN2	G3BP1	MRPL39
DHX9	RRM1	PSME3	MRPL16
TIMM8A	SARS	PSMD14	DARS2
DLAT	SDHC	POP7	IPO9
PHC1	SDHD	YAP1	RCC2
EEF2	SET	TIMM44	NUP107
EIF2S3	SLC2A1	RPP40	NLN
EIF4A1	SNRPA1	MRPS30	FAM60A
EIF4B	SNRPD1	RNPS1	TGIF2
FBL	SQLE	DBF4	MRPL11
FARSA	SSB	ERP29	C11orf48
FH	SS18	STIP1	WDR77
GARS	TCOF1	CBX3	C2orf47
GART	TERF1	MTF2	GEMIN6
HADH	TGIF1	NCBP2	PUS1
HDAC1	TP53	SEPHS2	TCF7L1
HNRNPA1	TRIP6	CCT5	PHF5A

PRMT1	UBE2G1	EXOSC7	MRPS36
HSPA9	UBE2V2	KPNA6	NUDCD2
KLF11	SUMO1	KLF4	
KPNA2	UGDH	LSM4	
KRAS	UQCRH	GNL3	
MCM7	VBP1	SNX5	
MSH2	WEE1	MRPS28	
MYC	XPO1	MRPS18B	
NASP	XRCC5	MRPL13	
NCL	YY1	MRPL15	

Table 6: WGCNA analysis of stemness related genes in xenograft mouse model CTCs and distribution of genes per expression module

Green module			
ALDOC	MSH2	TMEFF1	PIPOX
BIRC5	MYBL2	CCNB2	AMOTL2
ALDH7A1	NASP	EXO1	GTSE1
BLM	NCL	BUB3	DTL
BUB1	NEK2	AURKB	COQ3
BUB1B	NTHL1	TRIP13	MRPL39
CCNA2	PCNA	NCAPD2	ERCC6L
CCNC	PDCD2	CHAF1A	MRPL16
CCNF	PLK1	SMC4	CDCA8
CDC6	POLD1	G3BP1	DARS2
CDC20	POLE2	PRMT3	RCC2
CDC34	PPM1G	POP7	RAD18
CDKN3	PRIM1	NDC80	NUP107
RCC1	PRIM2	TIMM44	NLN
CHEK1	PRPS1	SMC2	FAM60A
CKS1B	RCN2	SPAG5	TGIF2
CKS2	RFC3	PLK4	MRPL11
CSE1L	RPA2	MTHFD2	WDR77
DLAT	RPA3	RPP40	C2orf47
DNMT1	RRM1	RUVBL2	GEMIN6
DTYMK	RRM2	MRPS30	ANP32E
E2F3	SDHD	RNPS1	CDCA3
ECHS1	SLC2A1	DBF4	CDCA7
EIF4EBP1	SLC16A1	WDHD1	THOC3
FBL	SNRPA	CHEK2	PHF5A
FARSA	SNRPA1	MTF2	CDCA5
GARS	SOX2	EXOSC7	NUDCD2
HADH	AURKA	NCAPH	
HELLS	TCF19	GSPT2	
HMGB2	TCOF1	LSM4	
PRMT1	TGIF1	CKAP2	
IARS	TOP2A	ACAD8	
KLF11	TP53	SNX5	
KPNA2	TTK	MRPL15	
KRAS	U2AF1	RACGAP1	
LMNB1	UBE2G1	GMNN	
MAD2L1	UGDH	MRPL4	

MCM2	VBP1	MRPS2	
MCM3	VRK1	MRTO4	
MCM4	WEE1	HN1	
MCM5	DEK	NUSAP1	
MCM7	CDC7	MRPL37	

Yellow module			
EEF2	PUS1		

Orange module			
ADSL	ELOVL6	RAB34	SARS
BCAT1	ENO1	RPL10A	TEAD2
CCND1	GJA1	RPL13	TIMM8B
CCND2	GNL3	RPL27A	TRIP6
CDKN1C	HDAC1	RPS12	WBP11
CSRP2	MID1IP1	RPS16	YAP1
CTSC	MYC	RPS19	ZNF22
EBNA1BP2	NAP1L1	RPS3	
EIF2S2	NIP7	RPS8	
EIF4A1	POLR2F	RPSA	

Purple module			
ABCB7	NDUFA9	SSB	NCBP2
ADH5	NDUFAB1	SS18	SEPHS2
PARP1	NDUFB7	TERF1	CCT5
SLC25A5	NDUFB8	UBE2V2	KPNA6
APEX1	NDUFS2	SUMO1	LSM5
ATP5J	NME2	UQCRH	KLF4
ATP5O	NME4	XPO1	TIMM13
BAX	NONO	XRCC5	PABPC1
BTF3	PA2G4	YY1	MRPS28
SERPINH1	PRDX1	DAP3	MRPS18B
COX5B	PDHA1	CLPP	MRPL13
CRABP2	PHB	NIPSNAP1	STOML2
CTNNA1	PPP4C	HAT1	UTP18
DHX9	MAPK13	RUVBL1	HSPA14
TIMM8A	PSMA5	BANF1	MRPS17
PHC1	PSMA7	DDX18	POLR3K
EIF2S3	PSMB5	EEF1E1	CYCS
EIF4B	PSMB6	PDIA4	IPO9
ETFA	RAD23B	GNA14	LSM2
FDPS	RPL22	GNPDA1	NT5DC2
FGFR1	RPS5	DPP3	C11orf48
FH	RPS23	PSME3	TCF7L1
GART	RPS27	PSMD14	FAM136A
GLO1	SDHC	LYPLA1	LSM10
HNRNPA1	SET	ERP29	MRPS36
HSPA9	SNRPD1	STIP1	NDUFA11
HSPE1	SQLE	CBX3	

CTC cluster dissociation

In order to identify actionable vulnerabilities of CTC clusters, and to test whether the epigenetic and transcriptional features of clustered CTCs are reversible upon cluster dissociation into single cells the following steps were undertaken. First, the expression of all known cell-cell junction (CCJ) components in patient samples obtained from normal breast (TGCA REF), breast cancer (TCGA REF), single CTCs and CTC clusters were assessed (Aceto et al. Cell 158, 1110-1122, 2014). While breast cancer cells tend to only partially reduce their CCJ repertoire compared to normal breast cells, CTCs express only a small fraction of CCJ components, likely as a consequence to their increased motility. Yet, CTC clusters retain a higher number of CCJs as compared to single CTCs. This analysis features a therapeutic opportunity, and demonstrates that CTC clusters rely upon a restricted number of CCJ components for their multicellular adhesion, with approaches aiming at dissociating them being able to spare normal tissues that express a higher variety of CCJs. To this end, 2'486 FDA-approved compounds were evaluated for their ability to dissociate clusters of human breast CTC-derived cells. Cluster dissociation was assessed using a high content screening microscope and comparing cells treated with each individual compound to steady state clustered BR16 cells and 40 µm-filtered BR16 single cell suspension as negative and positive controls, respectively (Fig. 4a). Interestingly, significant reduction in mean cluster size upon filtration did not affect viability but reduced mitochondrial membrane potential, as measured by tetramethylrhodamine methyl ester perchlorate (TMRM) intensity (Fig. 4a). For the majority of the 2'486 FDA-approved compounds, when using a 5 µM concentration for 2 days in hypoxic conditions, no detectable reduction in cell viability (>70% viability) nor mean cluster size (>450µm2) in BR16 CTC-derived cells was observed. Yet, 39 compounds were identified that significantly reduced mean cluster size without compromising viability. These compounds include inhibitors of Na^+/K^+ ATPases (n=6), HDACs (n=2), nucleotide biosynthesis (n=5), kinases (n=4), GPCRs (n=2), cholesterol biosynthesis (n=1), nuclear export (n=1), tubulin (n=9), as well as DNA binding compounds (n=8) and antibiotics (n=1). Reducing compound concentration to 1 µM, 0.5 µM and 0.1 µM resulted in a concomitant increase in mean cluster size of BR16 as well as BRx50 human CTC-derived cells (Fig. 4b). Along with the effects on cluster size, with a reduced compound concentration, an increase in the number of nuclei detected, mitochondrial membrane potential and overall viability for both cell lines was observed, indicating that cluster size correlates with overall fitness and proliferative ability of CTCs (Fig. 4b). Under these conditions, six compounds consistently led to a significant decrease in mean cluster size for both BR16 and Brx50 CTC cell lines, even at lowest concentrations tested (0.1 µM), namely the Na^+/K^+ ATPase inhibitors digitoxin and ouabain octahydrate, the tubulin binding agent podofilox (also known as podophyllotoxin), colchicine

and vincristine sulfate, and the tubulin binding agent and dual kinase inhibitor rigosertib (Fig. 4b).

Effect of CTC cluster dissociation on DNA methylation

In order to assess the effect of clustering on DNA methylation patterns and proliferation signature directly BR16 and BRx50 cell lines were cultured for 17 days to ensure that at least 4 divisions would take place. This is to allow proper time for DNA methylation remodeling to take place. Prolonged culture in the presence of 20 nM for the ATPase and kinase inhibitors was found to be optimal for cell proliferation and mean cluster size reduction (Fig. 5a) and on average n=20 cells in triplicate were further processed for WGBS and RNA-Seq.

Under these conditions, for both CTC derived cell lines, a subset of cluster-associated hypomethylated DMRs from patient and xenografts regain ≥20% methylation. Interestingly, this gain of methylation occurs in DMRs containing binding sites for stemness-related TFs, with ouabain treatment of BR16 cell line simultaneously affecting the binding sites of OCT4, SOX2 and NANOG. This indicates that the dissociation of CTC-clusters in patient-derived CTC lines leads to DNA remodeling that reduces the accessibility of binding sites for stemness-related TFs.

Table 7: NES score of TFBS identified in DMRs with ≥ 20% gain in methylation upon 17-day treatment of BR16 and BRx50 CTC cell line with 20 nM of Ouabain or Digitoxin. n=number of DMRs

	BR16		BRx50	
	Digitoxin (n=150)	Ouabain n=(108)	Digitoxin (n=124)	Ouabain (n=121)
ZNF274	-	4.59, 3.01	-	-
SUPT20H	-	-	-	-
YY2	-	6.5,	-	3.56
HMBOX1	-	3.89	3.749	3.35, 3.30, 3.22
HSF1	-	3.71	7.2	-
ZNF594	-	4.84	-	-
ABCF2	-	-	-	-
FOS	6.40, 3.63, 3.25	7.29, 6.04,	4.2, 3.4	3.91
ZNF493	-	-	3.88	3.12
ZKSCAN8	-	-	4.32	-
BDP1	4.18,	5.64	6.83	-
KDM5D	-	3.11	3.77	-
KDM5A	4.355	-	-	-
SP1	-	-	-	-
DND1	-	-	-	-
IRX3	5	3.63	-	-
STAT3	3.31	-	3.22	9.17, 3.80
ZNF92	3.44	-	-	-
ESR1	-	-	-	-
EZH2	4.63	-	-	-

LSM6	-	-	3.05	-
OCT4	-	3.2, 3.13	3.49, 3.40, 3.37	3.42
SIX4/5	-	6.27, 6.16	7.50, 7.47, 3.12	3.87, 3.65
CBFB	-	-	-	-
AGAP2	-	-	-	-
BCL11A	-	-	7.65	3.8, 3.69
LEF1	-	-	3.01	-
MEIS1	3.11	3	6.58, 3.02	4.09
RBMS1	-	-	-	-
TPPP	-	3.1	-	-
YAP5	5.4, 5.32, 4.56	3.55, 3.08	-	-
IRX6	5, 3.67	3.63	-	3.8
CF2-PA	-	-	-	-
ATOH1	-	-	-	-
ZNF207	-	-	-	-
SPI1	-	-	-	-
FOXG1/O1	3.61	3.74, 3.39	-	3.53, 3.25, 3.1
REX1	-	-	-	-
IRF4	-	3.244	-	-
SIN3A	-	-	-	-
NANOG	-	3.349, 3.28,	-	3.61
OCT4	-	3.204, 3.13	3.49, 3.4, 3.37	3.42
SOX2	3.22	4.82, 4.51, 4.24, 3.28	-	-
SR1	-	-	-	-
SOX18	3.99, 3.91	3.2	-	3.11
ZNF280A	-	-	-	-
CEBPD	3.76	4.05	-	-
POU1F1	-	-	4.02, 3.98	-
BHLHE40/4	-	-	4.61	-
BCL11A	-	-	7.65	3.8, 3.69
RORA	4.93, 3.45	-	-	4.02, 3.75
SRY	-	6.46, 6.36,	-	-
REST	-	-	4.85, 3.16, 3.11	-

Material and Methods

Cell Culture

CTC derived cells were maintained under hypoxia (5% oxygen) on ultra low attachment (ULA) 6-well plates (Corning, Cat# 3471-COR). CTC growth medium containing 20 ng/ml recombinant human Epidermal Growth Factor (Gibco, Cat# PHG0313), 20 ng/ml recombinant human Fibroblast Growth Factor (Gibco, Cat#100-18B), 1x B27 supplement (Invitrogen, Cat#17504-044) and 1x Antibiotic-Antimycotic (Invitrogen, Cat# 15240062) in RPMI 1640 Medium (Invitrogen, Cat# 52400-025) was added every third day. For passaging, cells were

spun down at 800 g for 5 min using a Heraeus Multifuge X3R centrifuge (Invitrogen, Cat#75004515). The supernatant was subsequently aspirated and cells were resuspended in 2 ml/well CTC medium and plated in 6-well ULA plates. BR 16 CTC-derived cells were generated in the inventors lab. Brx50 CTC-derived cells were obtained from the Haber and Maheswaran lab (MGH Cancer Center, Harvard Medical School, Boston, MA). MDA-MB-231 (LM2) cells were donated from Joan Massague's lab (MSKCC, New York, NY, USA) and passaged in DMEM/F-12 medium (Invitrogen, Cat#11330057) supplemented with 10% FBS (Invitrogen, Cat# 10500064) and 1x Antibiotic-Antimycotic (Invitrogen, Cat# 15240062). For passaging, LM2 cells were washed once with D-PBS (Invitrogen, Cat#14190169) and dissociated using 0.25% Trypsin (Invitrogen, Cat#25200056).

CTC Capture and Identification

Blood specimens for CTC analysis were obtained from University Hospital Basel after informed patient consent according to protocol EKNZ BASEC 2016-00067 and EK 321/10, which received ethical approval from the Swiss authorities (EKNZ, Ethics Committee northwest/central Switzerland). An average of 7.5 ml of blood per patient was drawn in EDTA vacutainers. Within 1 hr from blood draw, the blood was processed through Parsortix GEN3D6.5 Cell Separation Cassette (Angle Europe) according to the manufacturer's instructions. For mouse studies, blood was retrieved via cardiac puncture and 1 ml of blood was similarly processed through a Parsortix device. Captured CTCs were further stained on Parsortix cassette with EpCAM-AF488 conjugated (CellSignaling, Cat# CST5198), HER2-AF488 (#324410, BioLegend), EGFR-FITC conjugated (GeneTex, Cat# GTX11400) and CD45-BV605 conjugated (Biolegend, Cat# 304042 (anti-human); Cat# 103140 (anti-mouse)) antibodies.

Tumorigenesis Assays

All mouse experiments were carried out in compliance with institutional guidelines.

For tail vein experiments, NOD SCID Gamma (NSG) mice (Jackson Labs) were injected with $1x10^6$ BR16-mCherry cells resuspended in 100 µl D-PBS and monitored with IVIS Lumina II (Perkin Elmer). For CTC xenograft mouse model isolation, $1x10^6$ LM2-GFP, $1x10^6$ BRx50-GFP or $1x10^6$ BR16-GFP cells were resuspended in 100 µl of 50% Cultrex PathClear Reduced Growth Factor Basement Membrane Extract (R&D Biosystems, Cat# 3533-010-02) in D-PBS and injected orthotopically in NSG mice. Blood draw was performed 4-5 weeks after tumor onset for LM2 cells, 5-6 months after tumor onset for BR16 and 6-7 months after tumor onset for BRx50 cells.

Single-Cell Micromanipulation

Enriched CTCs were harvested from Parsortix cassette in 1 ml D-PBS solution (Invitrogen, Cat#14190169) in a 6-well ultra-low attachment plate (Corning, Cat# 3471-COR) and visualized using a CKX41 Olympus inverted fluorescent microscope (part of the AVISO CellCelector Micromanipulator –ALS). Single CTCs and CTC clusters were identified based on intact cellular morphology, AF488/FITC-positive staining and lack of BV605 staining. Target cells were individually micromanipulated with a 30 µM glass capillary on the AVISO CellCelector micromanipulator (ALS) and deposited into individual PCR tubes (Axygen, Cat#321-032-501) containing 10 µl of 2x Digestion Buffer (EZ DNA Methylation Direct Kit - Zymo, Cat# D5020) for WGBS or 2 µl of RLT lysis buffer (Qiagen, Cat#79216) supplemented with 1U/µl SUPERase In RNAse inhibitor (Invitrogen, Cat# AM2694) for RNA sequencing, and immediately flash frozen in liquid nitrogen.

Single Cell Whole-genome Bisulfite Sequencing

Proteinase K digestion and bisulfite treatment was performed according to manufacturer's instructions for EZ DNA Methylation Direct Kit (Zymo, Cat# D5020). Bisulfite-treated DNA was eluted using 9 µl of Elution Buffer and used for library generation with TruSeq DNA methylation kit (Illumina, Cat# EGMK91396) according to manufacturer's instructions. For amplification, 18 cycles were performed using Failsafe Enzyme (Illumina, Cat# FSE51100) and indexes were introduced with Index Primers' Kit (Illumina, Cat# EGIDX81312). Library purification was performed using Agencourt AMPure XP beads at a ratio of 1:1 according to manufacturer's instructions. To avoid DNA loss during pipetting steps, Corning DeckWork low binding barrier pipet tips were used (Sigma, Cat# CLS4135-4X960EA). Library concentration was estimated using Qubit DS DNA HS Assay Kit according to manufacturer's instructions (Invitrogen, Cat#Q32854).

RNA-Seq Library generation

RNA was captured on beads conjugated with oligo-dT primer according to Macaulay et al. (Nat Protoc 11, 2081-2103, 2016). cDNA was generated according to Picelli at al.'s Smart-Seq 2 protocol (Nat Protoc 9, 171-181, 2014). Sequencing libraries were generated and indexed from 0.25 ng of cDNA per sample using the Nextera XT DNA Library Preparation Kit (Illumina, Cat# FC-131-2001) according to manufacturer's instructions

FDA-Approved Compound Screen

A library containing 2,486 FDA-approved compounds was purchased from the Nexus Platform – ETH Zurich. Each compound was resuspended using CTC medium at a 15 µM concentration and 20 µl were aliquoted in duplicate in a total of 64 Flat Bottom Clear Ultra Low attachment 96-well plates (Corning, Cat#3474).

To reduce cluster size in CTC derived cell lines, a 40 µm cell strainer was used (Corning, Cat# 431750). 40 µl containing 5'000 CTC-derived cells were seeded per well in 96-well ultra low attachment plates that contained 20 µl of pre-aliquoted FDA-approved compounds at 15 µM concentration, so that final compound concentration was 5 µM. Plates were incubated in hypoxia (5% oxygen) for 2 days and then 20 µl were transferred into a 96 well Black/clear Tissue culture treated plate (BD Falcon, Cat#353219) containing 40 µl of D-PBS (Invitrogen, Cat#14190169) and stained for 1hr at 37°C with a final concentration of 4 µM Hoechst 34580 (Invitrogen, Cat# H21486), 2 µM TMRM (Invitrogen, Cat#T668) and 4 µM TOTO-3 (Invitrogen, Cat# T3604). For each plate, two positive controls (non-treated cells) and two negative controls (non-treated and 40 µM-filtered cells) were included. Z-factors were calculated per individual plate using the following formula: $Z'=1-3(\sigma_s + \sigma_c)/|\mu_s-\mu_c|^3$ (σ: standard deviation, μ: mean, s: positive control and c: negative control) (Martin et al., PLoS One 9, e88338, 2014) and ranged between 0.62-0.937. Plates were scanned using Operetta High Content Imaging System (Perkin Elmer) and cluster analysis was performed using Harmony High Content Imaging and Analysis Software (Perkin Elmer).

Enrichment scores

An enrichment score (ES) indicates the over- or underrepresentation of a certain object within a sample of many objects (=enrichment). A positive ES indicates that a certain feature is overrepresented as compared to other features within an analysed set of features (=enrichment). A negative enrichment score indicates the opposite, namely that a feature is less present than to be expected by the values of other features in the sample. In other words, a positive ES for a transcription factor binding site (TFBS) indicates that the TFBS is represented in the sample to a higher degree than other TFBS (=enriched). An enrichment score can be normalized by dividing a specific ES by the mean of the enrichment scores for all objects in the dataset to yield a normalized enrichment score (NES). Normalization of the enrichment score accounts for differences in gene set size and in correlations between gene sets and the expression dataset; therefore, a normalized enrichment scores (NES) can be used to compare analysis results across gene sets. Only TFBS with a NES score ≥3.0 are considered significant shown in the analysis.

CRISPR-CAS9 CLDN3/4 Double knock out in BR16

The inventors used lentiviral delivery of pLenti-Cas9-EGFP vector (Addgene) to generate a BR16 CTC-derived cell line that stably expresses the Cas9 protein together with GFP. In BR16-Cas9-GFP line the inventors then introduced sgRNA sequences that target either CLDN3 or CLDN4. In detail, sgRNA sequences were designed using the GPP Web Portal (https://portals.broadinstitute.org/gpp/public/analysis-tools/sgrna-design). Two sgRNAs targeting CLDN3 ((sense) 5'-CACGTCGCAGAACATCTGGG-3' (SEQ ID NO 001) and (sense)

5'-ACGTCGCAGAACATCTGGGA-3' SEQ ID NO 002)) were cloned in vector pLentiGuide-Puro (Addgene) and 2 sgRNAs targeting CLDN4 ((sense) 5'-CAAGGCCAAGACCATGATCG-3' (SEQ ID NO 003) and (sense) 5'-ATGGGTGCCTCGCTCTACGT-3' (SEQ ID NO 004)) were cloned in vector pLentiGuide-Blast. Vector pLentiGuide-Blast was generated by replacing puromycin resistance gene on plasmid pLentiGuide-Puro with the blasticidin resistance gene using the MluI and BsiWI restriction enzyme sites. Double positive-clones were selected based on puromycin (1µg/mL) and blasticidin (10µg/mL) antibiotic selection for 2 weeks and CLDN3/CLDN4 knockout was verified by western blot.

Claims

1. A tubulin inhibitor for use in the prevention or treatment of metastasis in a cancer patient, particularly a patient characterized by the presence of CTC clusters in the bloodstream.

2. The tubulin inhibitor for use in the prevention or treatment of metastasis according to claim 1, wherein the tubulin inhibitor is selected from a tubulin polymerization inhibitor and a tubulin depolymerization inhibitor.

3. The tubulin inhibitor for use in the prevention or treatment of metastasis according to any one of claims 1 or 2, wherein the tubulin polymerization inhibitor is selected from a vinca domain binding inhibitor and a colchicine domain binding inhibitor.

4. The tubulin inhibitor for use in the prevention or treatment of metastasis according to claim 3, wherein
   a) the vinca domain binding inhibitor is selected from: vincristine, vinblastine, vinorelbine, vinflunine, cryptophycin 52, halichondrins, dolastatins and hemiasterlines, in particular vincristine;
   and/or
   b) the colchicine domain binding inhibitor is selected from: colchicine, podophyllotoxin, rigosertib, steganacin, ABT-751, combretastatin, fenbendazole, oxibendazole, albendazole and 2-methoxyestradiol, in particular colchicine, podophyllotoxin, rigosertib, fenbendazole, oxibendazole and albendazole.

5. The tubulin inhibitor for use in the prevention or treatment of metastasis according to any one of claims 1 or 2, wherein the tubulin depolymerization inhibitor is selected from a taxan domain binding inhibitor and a laulimalide binding inhibitor.

6. The tubulin inhibitor for use in the prevention or treatment of metastasis according to claim 5, wherein
   a) the taxan domain binding inhibitor is selected from paclitaxel, docetaxel, epothilone and discodermolide, in particular paclitaxel;
   and/or
   b) the laulimalide binding inhibitor is selected from laulimalide and peloruside A.

7. The tubulin inhibitor for use in the prevention or treatment of metastasis according to any one of the above claims, wherein the tubulin inhibitor is effective in the disruption of CTC clusters.

8. The tubulin inhibitor for use in the prevention or treatment of metastasis according to any one of the above claims, wherein the tubulin inhibitor additionally comprises a dual kinase inhibitory activity, in particular an inhibition of the PI3K and PLK1 pathway.

9. The tubulin inhibitor for use in the prevention or treatment of metastasis additionally comprising a dual kinase inhibitory activity according to claim 8, wherein the tubulin inhibitor is rigosertib.

10. A tubulin inhibitor according to any one of claims 1 to 9 for use in the prevention and treatment of venous thromboembolism in cancer patients.

Fig. 1

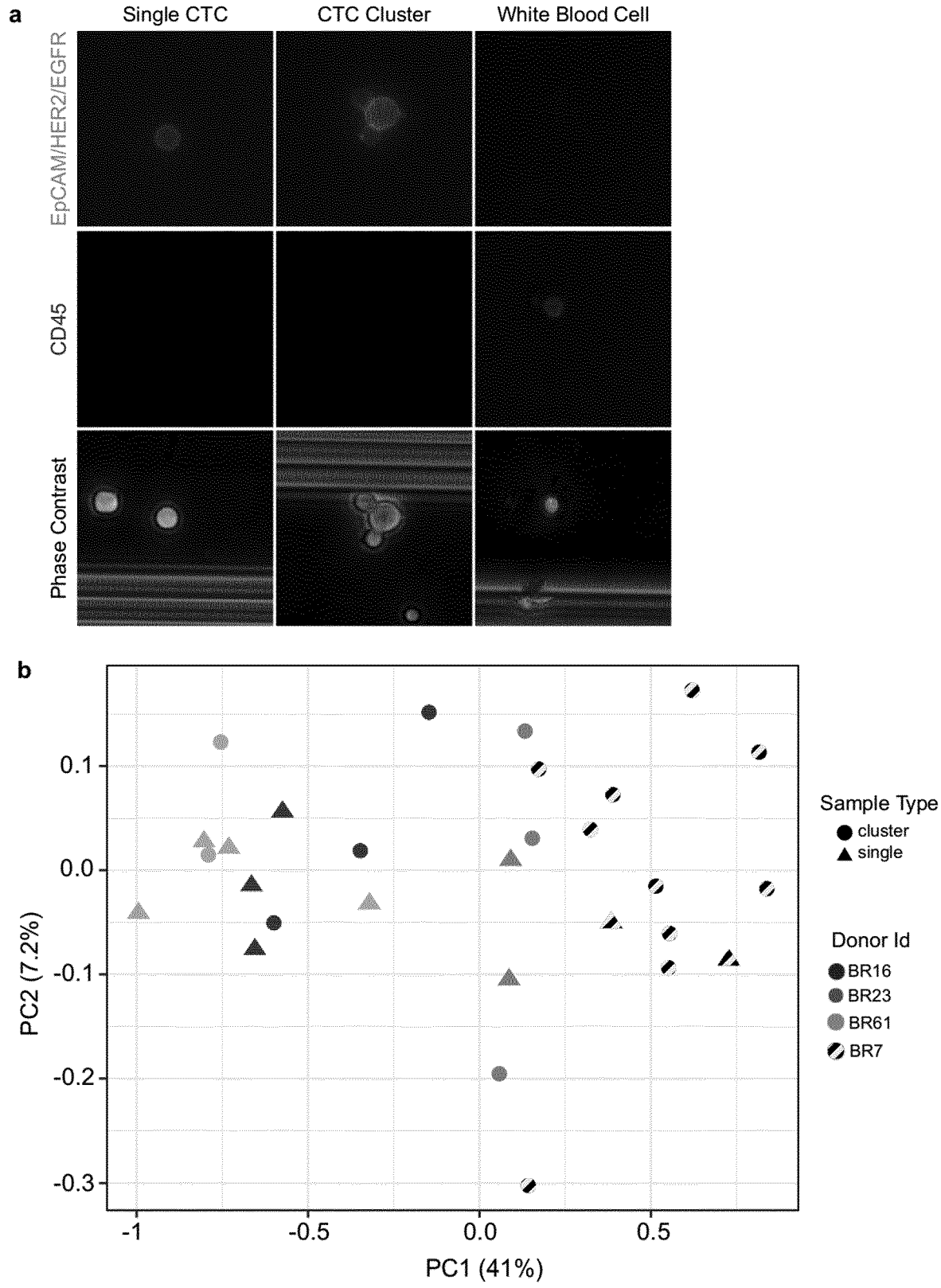
a
Single CTC
CTC Cluster
White Blood Cell
EpCAM/HER2/EGFR
CD45
Phase Contrast
b
PC2 (7.2%)
PC1 (41%)
0.1
0.0
-0.1
-0.2
-0.3
-1
-0.5
0.0
0.5
Sample Type
cluster
single
Donor Id
BR16
BR23
BR61
BR7

Fig. 1 continued

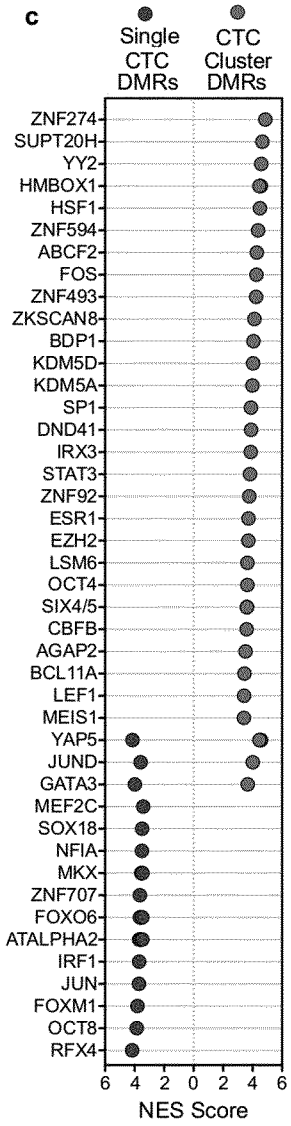

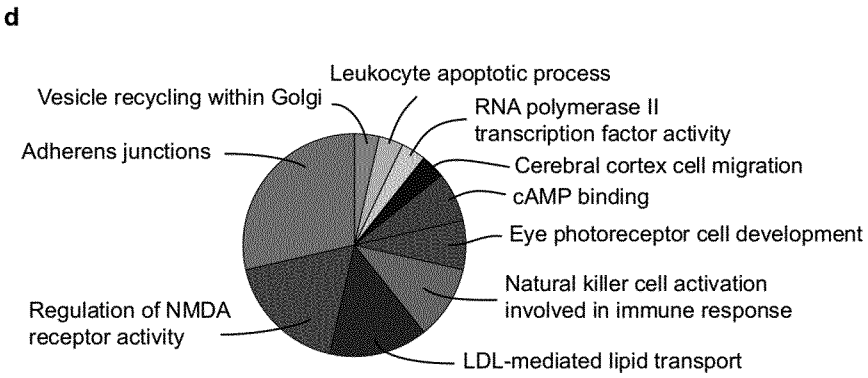

Fig. 2

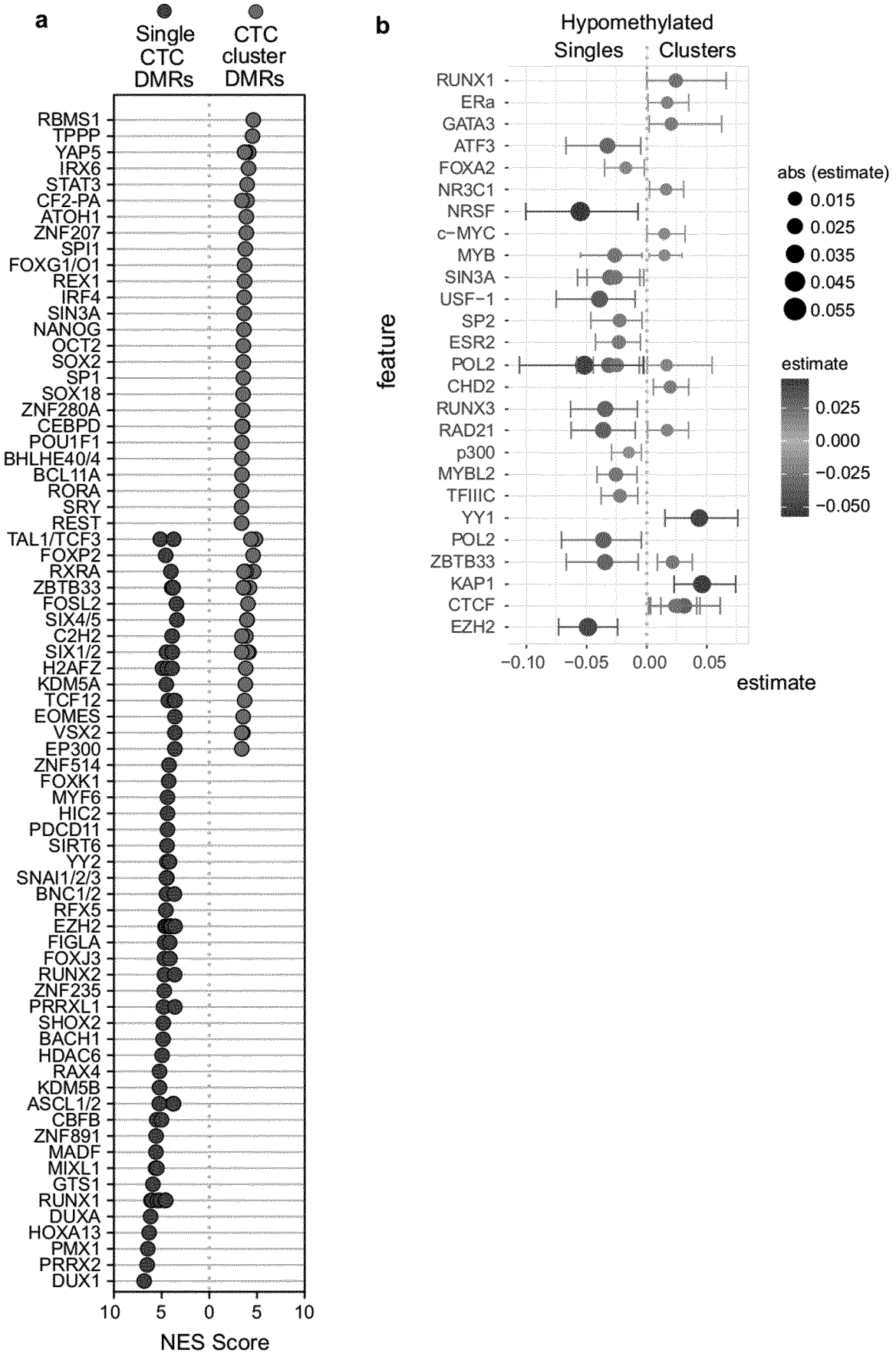
a
Single CTC DMRs
CTC cluster DMRs
RBMS1
TPPP
YAP5
IRX6
STAT3
CF2-PA
ATOH1
ZNF207
SPI1
FOXG1/O1
REX1
IRF4
SIN3A
NANOG
OCT2
SOX2
SP1
SOX18
ZNF280A
CEBPD
POU1F1
BHLHE40/4
BCL11A
RORA
SRY
REST
TAL1/TCF3
FOXP2
RXRA
ZBTB33
FOSL2
SIX4/5
C2H2
SIX1/2
H2AFZ
KDM5A
TCF12
EOMES
VSX2
EP300
ZNF514
FOXK1
MYF6
HIC2
PDCD11
SIRT6
YY2
SNAI1/2/3
BNC1/2
RFX5
EZH2
FIGLA
FOXJ3
RUNX2
ZNF235
PRRXL1
SHOX2
BACH1
HDAC6
RAX4
KDM5B
ASCL1/2
CBFB
ZNF891
MADF
MIXL1
GTS1
RUNX1
DUXA
HOXA13
PMX1
PRRX2
DUX1
10 5 0 5 10
NES Score
b
Hypomethylated
Singles
Clusters
feature
RUNX1
ERa
GATA3
ATF3
FOXA2
NR3C1
NRSF
c-MYC
MYB
SIN3A
USF-1
SP2
ESR2
POL2
CHD2
RUNX3
RAD21
p300
MYBL2
TFIIIC
YY1
POL2
ZBTB33
KAP1
CTCF
EZH2
−0.10 −0.05 0.00 0.05
estimate
abs (estimate)
0.015
0.025
0.035
0.045
0.055
estimate
0.025
0.000
−0.025
−0.050

Fig. 3

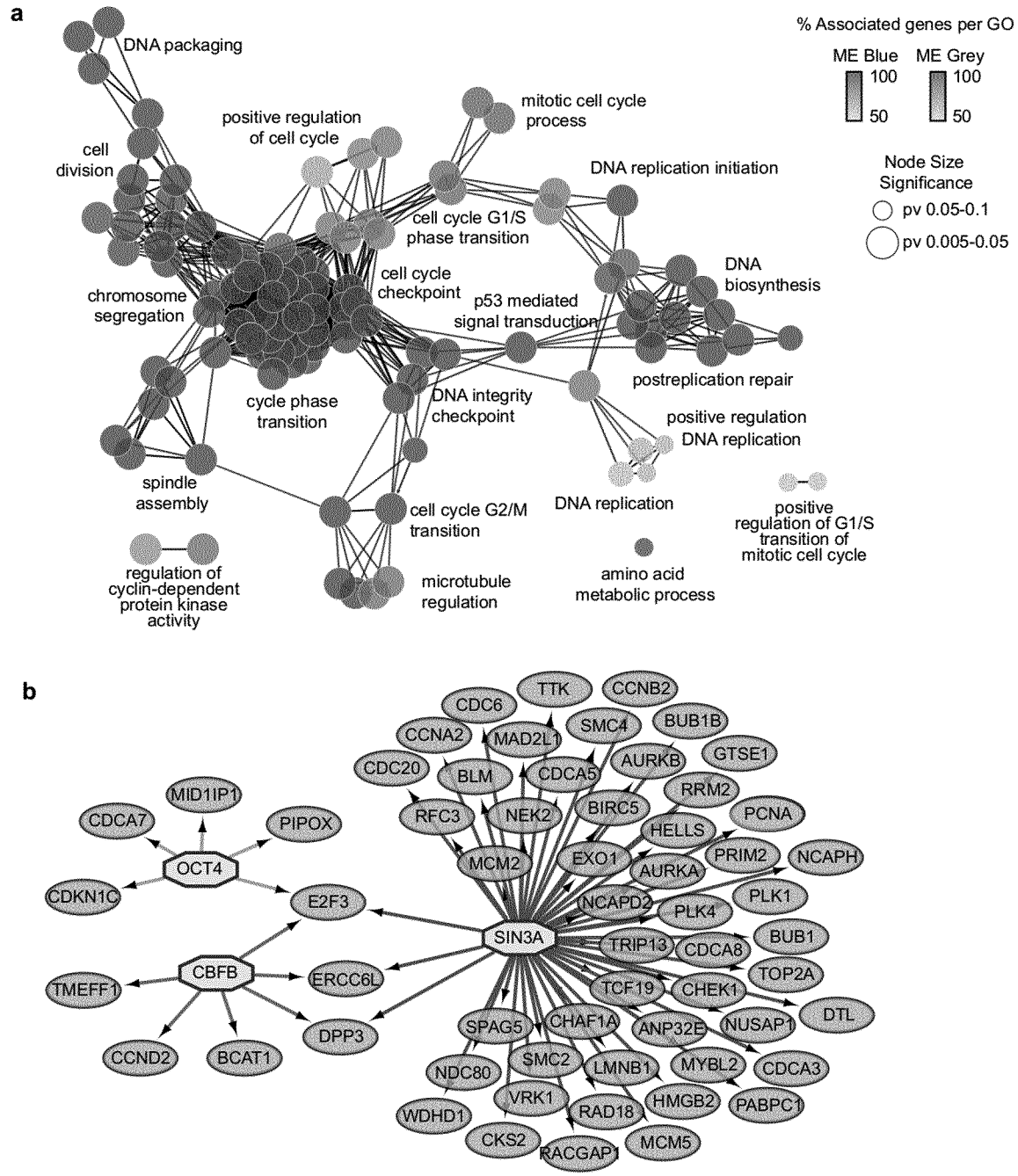
a
% Associated genes per GO
ME Blue
100
50
ME Grey
100
50
Node Size
Significance
pv 0.05-0.1
pv 0.005-0.05
DNA packaging
positive regulation of cell cycle
mitotic cell cycle process
cell division
DNA replication initiation
cell cycle G1/S phase transition
cell cycle checkpoint
DNA biosynthesis
chromosome segregation
p53 mediated signal transduction
postreplication repair
cycle phase transition
DNA integrity checkpoint
positive regulation DNA replication
spindle assembly
cell cycle G2/M transition
DNA replication
positive regulation of G1/S transition of mitotic cell cycle
regulation of cyclin-dependent protein kinase activity
microtubule regulation
amino acid metabolic process
b
TTK
CCNB2
CDC6
SMC4
BUB1B
CCNA2
MAD2L1
GTSE1
AURKB
CDC20
BLM
CDCA5
RRM2
RFC3
NEK2
BIRC5
PCNA
HELLS
MID1IP1
CDCA7
PIPOX
MCM2
EXO1
PRIM2
NCAPH
AURKA
OCT4
CDKN1C
E2F3
NCAPD2
PLK1
PLK4
SIN3A
TRIP13
CDCA8
BUB1
CBFB
TOP2A
TMEFF1
ERCC6L
TCF19
CHEK1
DTL
SPAG5
CHAF1A
ANP32E
NUSAP1
DPP3
CCND2
BCAT1
SMC2
LMNB1
MYBL2
CDCA3
NDC80
VRK1
RAD18
HMGB2
PABPC1
WDHD1
CKS2
MCM5
RACGAP1

Fig. 3 continued

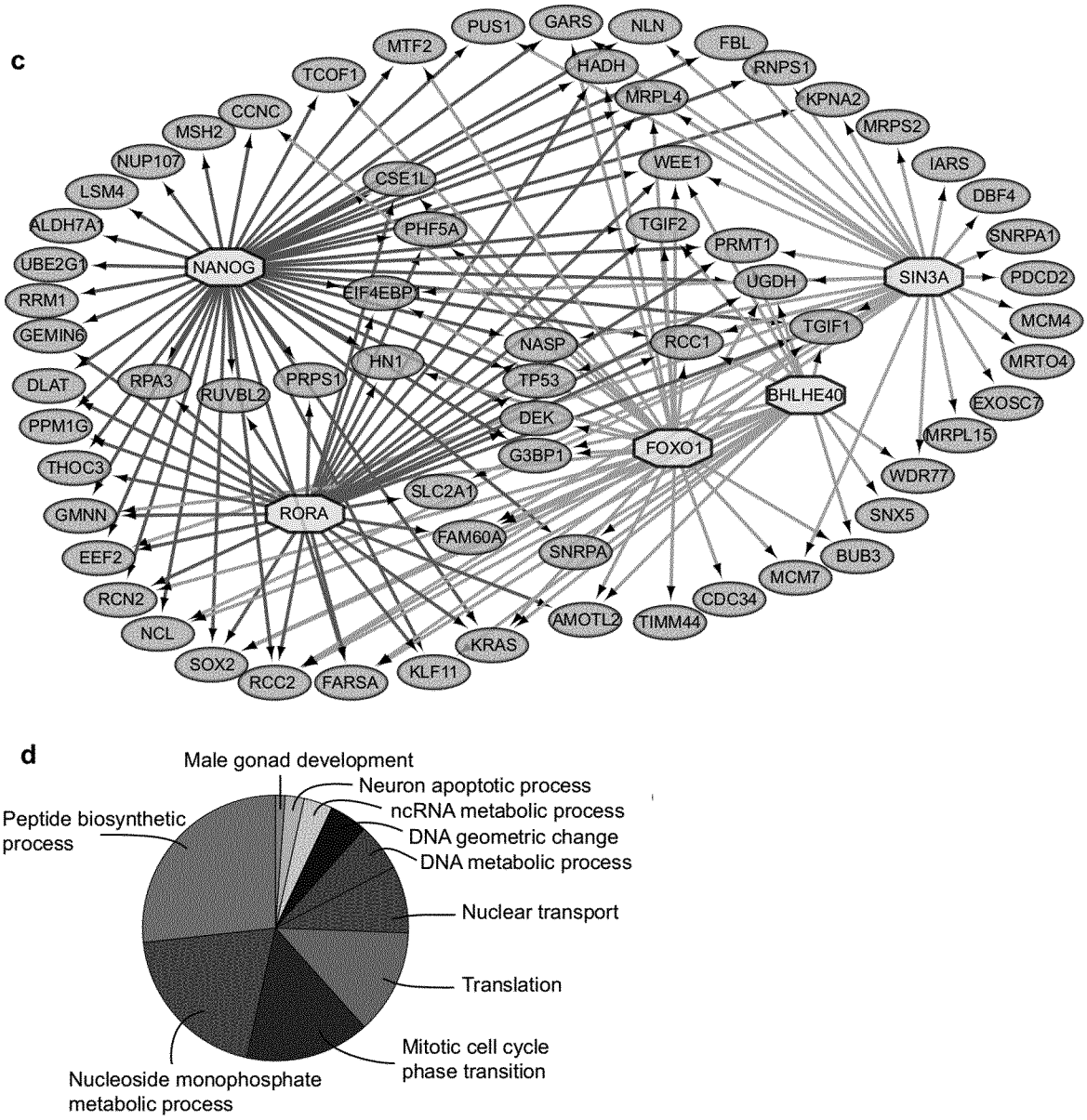

Fig. 3 continued

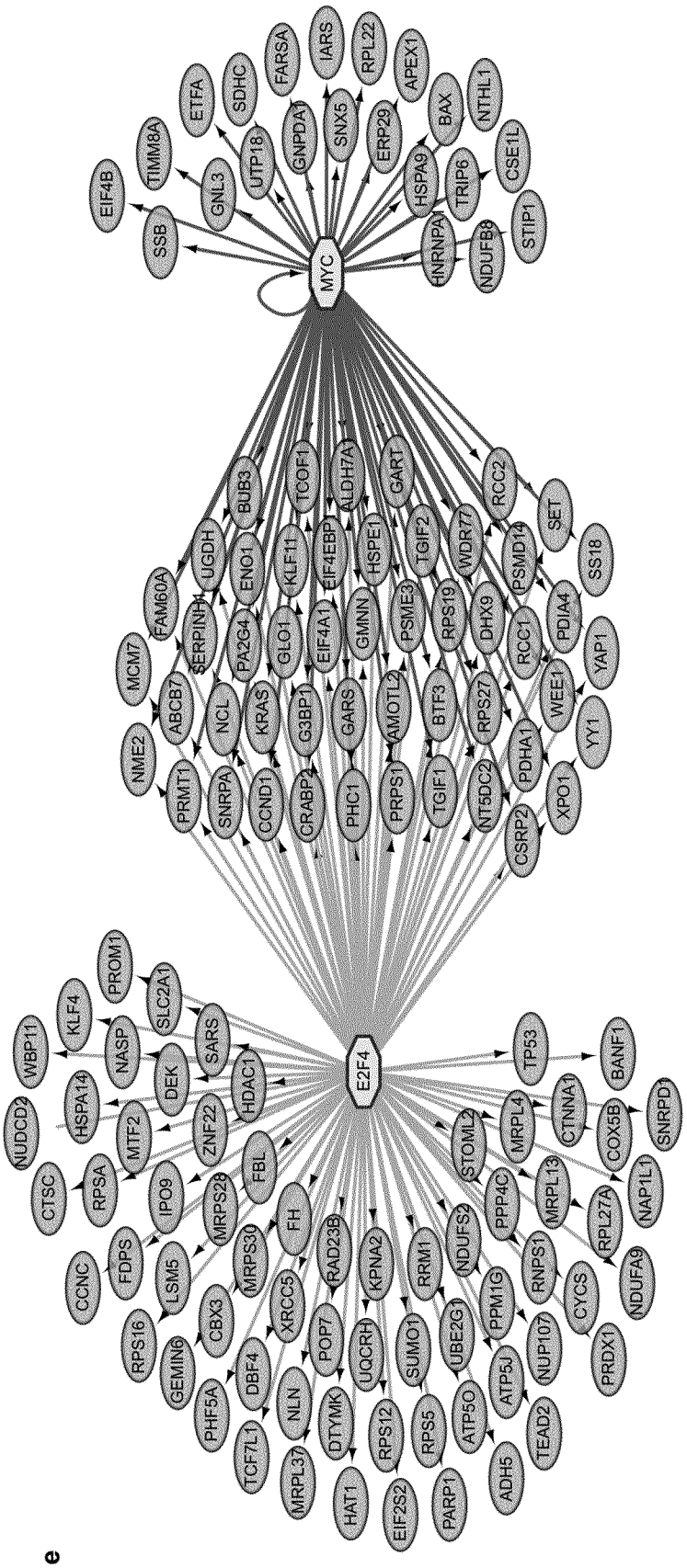

e

Fig. 4

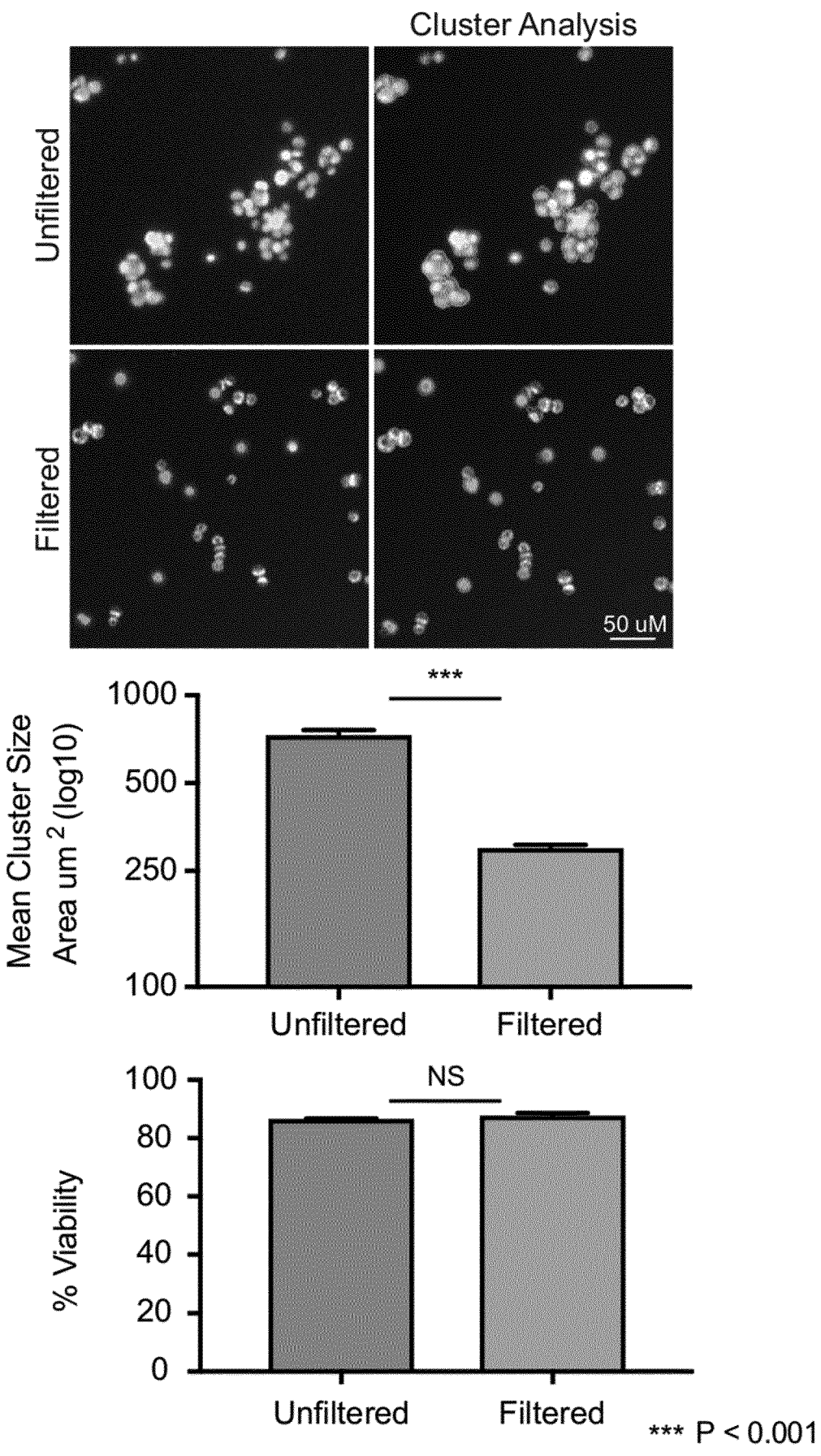
a
Cluster Analysis
Unfiltered
Filtered
50 uM
***
Mean Cluster Size
Area um 2 (log10)
1000
500
250
100
Unfiltered
Filtered
NS
% Viability
100
80
60
40
20
0
Unfiltered
Filtered
*** P < 0.001

Fig. 4 continued

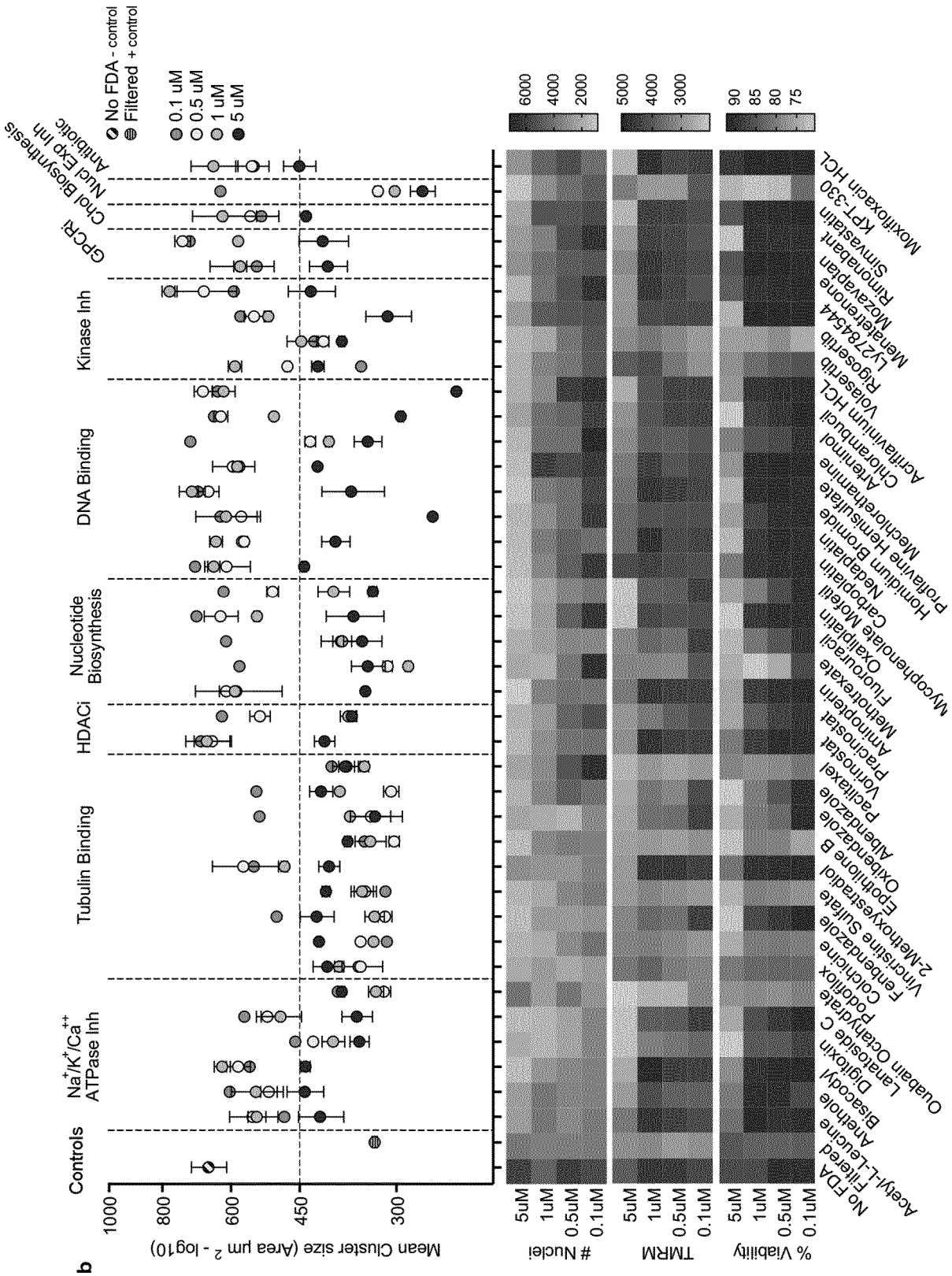

Fig. 5

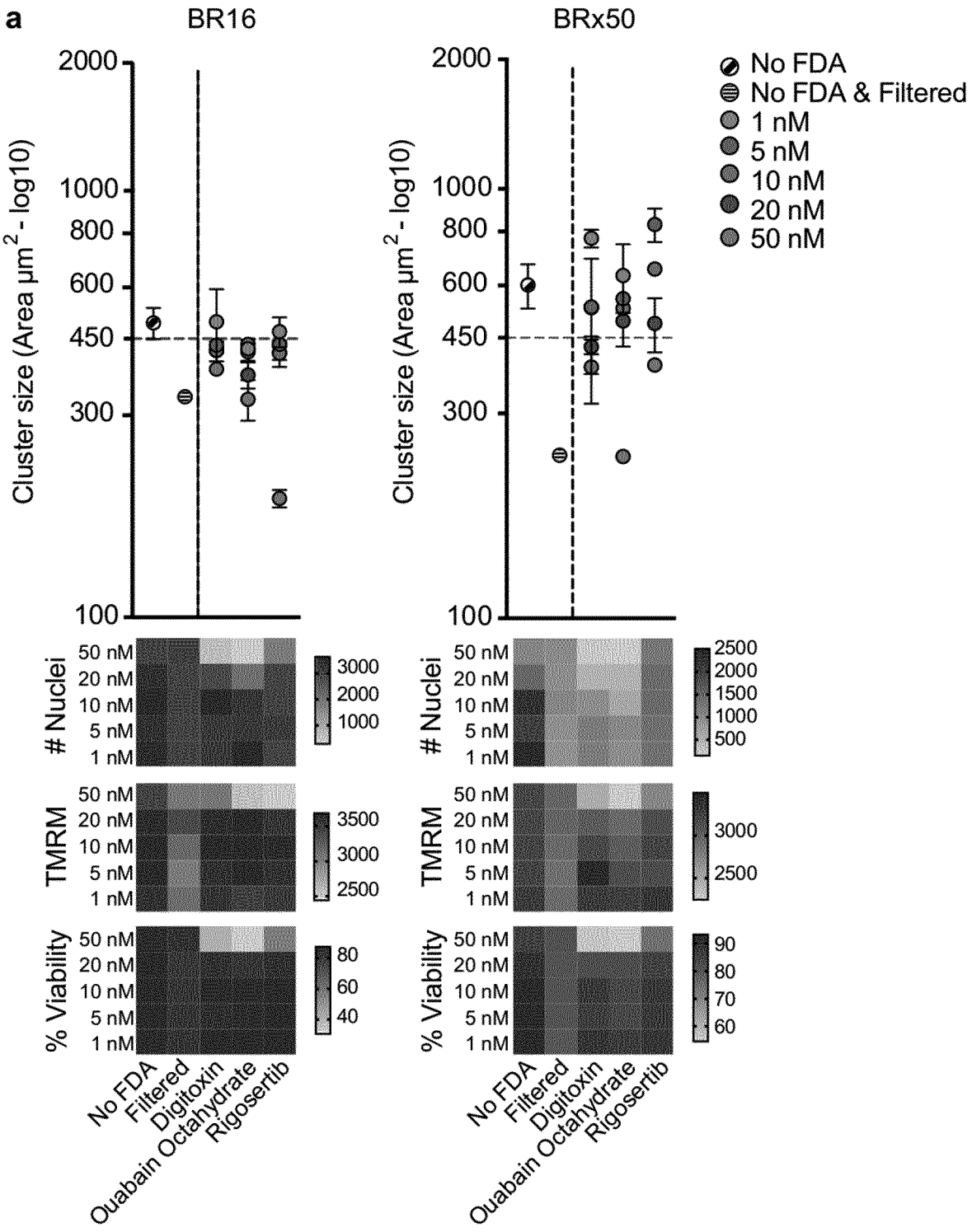
a
BR16
BRx50
No FDA
No FDA & Filtered
1 nM
5 nM
10 nM
20 nM
50 nM
Cluster size (Area µm2 - log10)
2000
1000
800
600
450
300
100
Nuclei
TMRM
% Viability
50 nM
20 nM
10 nM
5 nM
1 nM
3000
2000
1000
2500
1500
500
3500
2500
80
60
40
90
70
No FDA
Filtered
Digitoxin
Ouabain Octahydrate
Rigosertib

Fig. 6

A

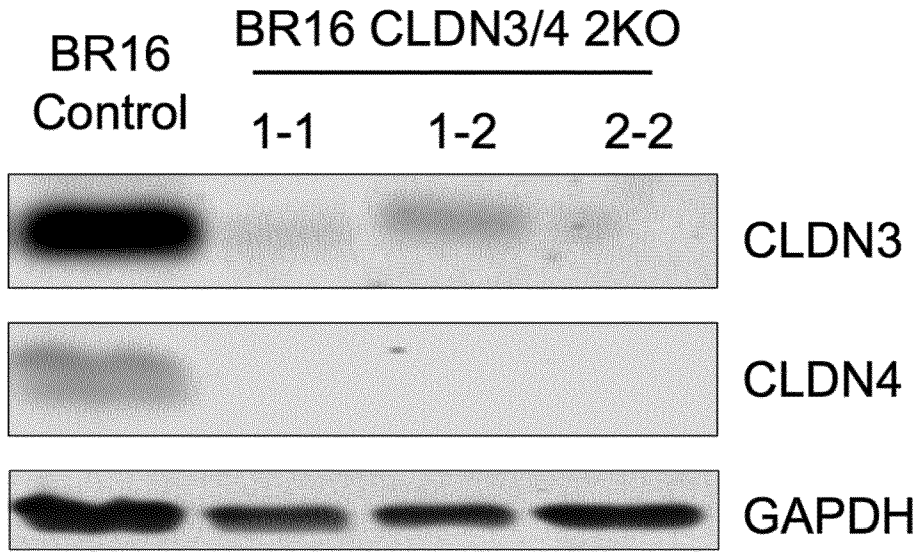
BR16 Control
BR16 CLDN3/4 2KO
1-1
1-2
2-2
CLDN3
CLDN4
GAPDH

B

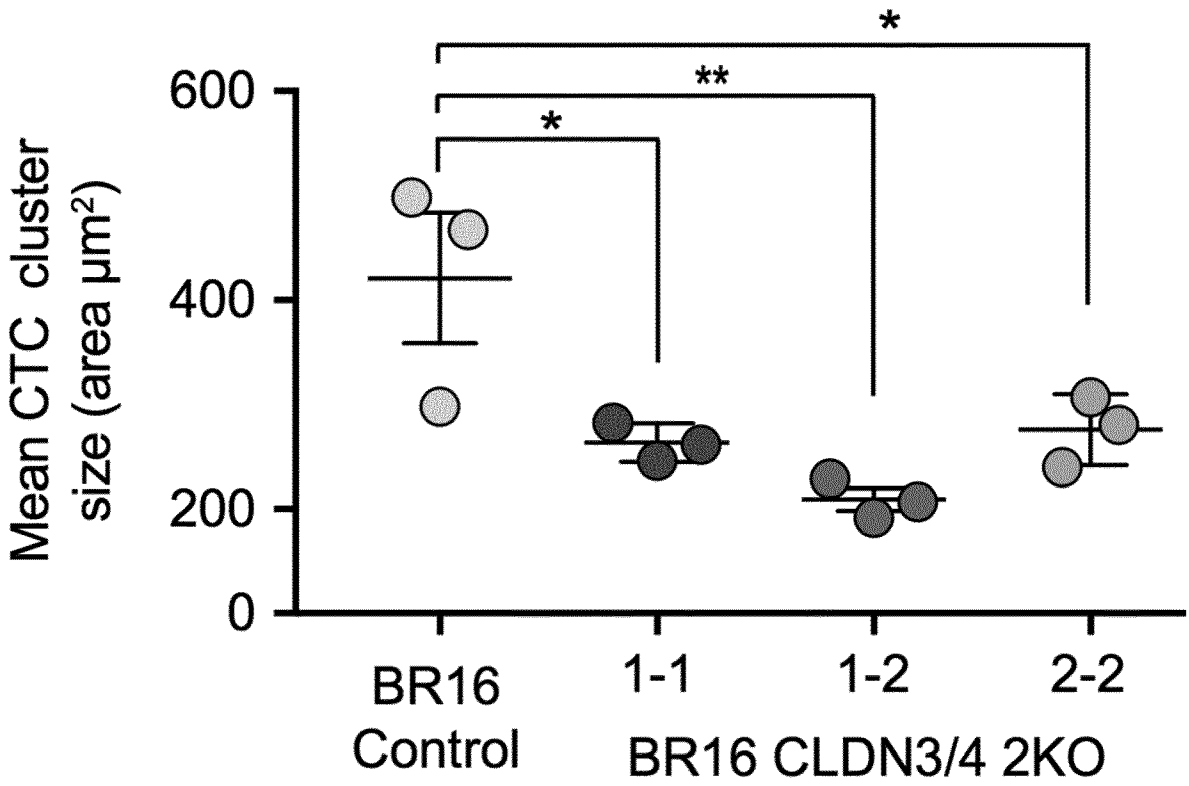
Mean CTC cluster size (area µm²)
600
400
200
0
*
**
*
BR16 Control
1-1
1-2
2-2
BR16 CLDN3/4 2KO